



Measurement of prompt photon production in root $s(\text{NN})=8.16$ TeV p Pb collisions with ATLAS

Aaboud, M.; Aad, G.; Abbott, B.; Abbott, DC; Abdinov, O.; Abeloos, B; Abhayasinghe, DK; Abidi, S.H.; AbouZeid, Ossama Sherif Alexander; Abraham, NL; Bajic, Milena; Besjes, Geert-Jan; Alonso Diaz, Alejandro; Camplani, Alessandra; Dam, Mogens; de Almeida Dias, Flavia; hqz214, hqz214; Galster, Gorm Aske Gram Krohn; Hansen, Jørn Dines; Hansen, Peter Henrik; Hansen, Jørgen Beck; Ignazzi, Rosanna; Monk, James William; Petersen, Troels Christian; Stark, Simon Holm; Xella, Stefania; Wigglesworth, Graig; ATLAS

Published in:
Physics Letters B

DOI:
[10.1016/j.physletb.2019.07.031](https://doi.org/10.1016/j.physletb.2019.07.031)

Publication date:
2019

Document version
Publisher's PDF, also known as Version of record

Citation for published version (APA):
Aaboud, M., Aad, G., Abbott, B., Abbott, DC., Abdinov, O., Abeloos, B., Abhayasinghe, DK., Abidi, S. H., AbouZeid, O. S. A., Abraham, NL., Bajic, M., Besjes, G-J., Alonso Diaz, A., Camplani, A., Dam, M., de Almeida Dias, F., hqz214, H., Galster, G. A. G. K., Hansen, J. D., ... ATLAS (2019). Measurement of prompt photon production in root $s(\text{NN})=8.16$ TeV p Pb collisions with ATLAS. *Physics Letters B*, 796, 230-252.
<https://doi.org/10.1016/j.physletb.2019.07.031>



Measurement of prompt photon production in $\sqrt{s_{NN}} = 8.16$ TeV $p + \text{Pb}$ collisions with ATLAS

The ATLAS Collaboration*



ARTICLE INFO

Article history:

Received 7 March 2019

Received in revised form 19 June 2019

Accepted 15 July 2019

Available online 17 July 2019

Editor: M. Doser

ABSTRACT

The inclusive production rates of isolated, prompt photons in $p + \text{Pb}$ collisions at $\sqrt{s_{NN}} = 8.16$ TeV are studied with the ATLAS detector at the Large Hadron Collider using a dataset with an integrated luminosity of 165 nb^{-1} recorded in 2016. The cross-section and nuclear modification factor $R_{p\text{Pb}}$ are measured as a function of photon transverse energy from 20 GeV to 550 GeV and in three nucleon–nucleon centre-of-mass pseudorapidity regions, $(-2.83, -2.02)$, $(-1.84, 0.91)$, and $(1.09, 1.90)$. The cross-section and $R_{p\text{Pb}}$ values are compared with the results of a next-to-leading-order perturbative QCD calculation, with and without nuclear parton distribution function modifications, and with expectations based on a model of the energy loss of partons prior to the hard scattering. The data disfavour a large amount of energy loss and provide new constraints on the parton densities in nuclei.

© 2019 The Author. Published by Elsevier B.V. This is an open access article under the CC BY license (<http://creativecommons.org/licenses/by/4.0/>). Funded by SCOAP³.

1. Introduction

Measurements of particle and jet production rates at large transverse energy are a fundamental method of characterising hard-scattering processes in all collision systems. In collisions involving large nuclei, production rates are modified from those measured in proton + proton (pp) collisions due to a combination of initial- and final-state effects. The former arise from the dynamics of partons in the nuclei prior to the hard-scattering process, while the latter are attributed to the strong interaction of the emerging partons with the hot nuclear medium formed in nucleus–nucleus collisions. Modification due to the nuclear environment is quantified by the nuclear modification factor, R_{AA} , defined as the ratio of the cross-section measured in $A + A$ to that in pp collisions, scaled by the expected geometric difference between the systems.

Measurements of prompt photon production rates offer a way to isolate the initial-state effects because the final-state photons do not interact strongly. These initial-state effects include the degree to which parton densities are modified in a nuclear environment [1–3], as well as potential modification due to an energy loss arising through interactions of the partons traversing the nucleus prior to the hard scattering [4,5]. Constraints on such initial-state effects are particularly important for characterising the observed modifications of strongly interacting final states, such as jet and hadron production [6,7], since they are sensitive to effects

from both initial- and final-state. Due to the significantly simpler underlying-event conditions in proton–nucleus collisions, measurements of photon rates can be performed with better control over systematic uncertainties than in nucleus–nucleus collisions, allowing a more precise constraint on these initial-state effects.

Prompt photon production has been extensively measured in pp collisions at a variety of collision energies [8–12] at the Large Hadron Collider (LHC). It was also measured in lead–lead ($\text{Pb}+\text{Pb}$) collisions at a nucleon–nucleon centre-of-mass energy $\sqrt{s_{NN}} = 2.76$ TeV [13,14] at the LHC, and in gold–gold collisions at $\sqrt{s_{NN}} = 200$ GeV at the Relativistic Heavy Ion Collider (RHIC) [15], where the data from both colliders indicate that photon production rates are unaffected by the passage of the photons through the hot nuclear medium. At RHIC, photon production rates were measured in deuteron–gold collisions at $\sqrt{s_{NN}} = 200$ GeV [16,17] and were found to be in good agreement with perturbative QCD (pQCD) calculations. Additionally, jet production [18,19] and electroweak boson production [20–22] were measured in 28 nb^{-1} of proton–lead ($p + \text{Pb}$) collision data at $\sqrt{s_{NN}} = 5.02$ TeV recorded at the LHC; the former is a strongly interacting final state, while the latter is not. All measurements provided some constraints on initial-state effects.

The data used in this measurement were collected with the ATLAS detector during the $p + \text{Pb}$ collision running period in 2016, and correspond to an integrated luminosity of 165 nb^{-1} , approximately six times larger than the measurements made in the previous 5.02 TeV data. The proton and lead beams had an energy of 6.5 TeV and 2.51 TeV per nucleon respectively, resulting in a nucleon–nucleon centre-of-mass collision energy of 8.16 TeV and

* E-mail address: atlas.publications@cern.ch.

a rapidity boost of this frame by ± 0.465 units relative to the ATLAS laboratory frame, depending on the direction of the Pb beam.¹ By convention, the results are reported as a function of photon pseudorapidity in the nucleon–nucleon collision frame, η^* , with positive η^* corresponding to the proton beam direction, and negative η^* corresponding to the Pb beam direction.

At leading order, the process $p + \text{Pb} \rightarrow \gamma + X$ has contributions from direct processes, in which the photon is produced in the hard interaction, and from fragmentation processes, in which it is produced in the parton shower. Beyond leading order the direct and fragmentation components are not separable and only their sum is a physical observable.

To reduce contamination from the dominant background of photons mainly from light-meson decays in jets, the measurements presented here require the photons to be isolated from nearby particles. This requirement also acts to reduce the relative contribution of fragmentation photons in the measurement, and thus, the same fiducial requirement must be imposed on theoretical models when comparing with the data. Specifically, as in previous ATLAS measurements [9,10], the sum of energy transverse to the beam axis within a cone of $\Delta R \equiv \sqrt{(\Delta\eta)^2 + (\Delta\phi)^2} = 0.4$ around the photon, E_T^{iso} , is required to be smaller than $4.8 + 4.2 \times 10^{-3} E_T^\gamma$ [GeV], where E_T^γ is the transverse energy of the photon. At particle level, E_T^{iso} is calculated as the sum of transverse energy of all particles with a decay length above 10 mm, excluding muons and neutrinos. This sum is corrected for the ambient contribution from underlying-event particles, consistent with the previous measurements [9,10].

This letter reports a measurement of the cross-section for prompt, isolated photons in $p + \text{Pb}$ collisions at $\sqrt{s_{\text{NN}}} = 8.16$ TeV. Photons are measured with $E_T^\gamma > 20$ GeV, the isolation requirement detailed above, and in three nucleon–nucleon centre-of-mass pseudorapidity (η^*) regions, $-2.83 < \eta^* < -2.02$, $-1.84 < \eta^* < 0.91$, and $1.09 < \eta^* < 1.90$. In addition to the cross-section, the data are compared to a pp reference cross-section derived from a previous measurement of prompt photon production in pp collisions at $\sqrt{s} = 8$ TeV that used the identical isolation condition [9]. The nuclear modification factor $R_{p\text{Pb}}$ is derived in each pseudorapidity region, using an extrapolation for the different collision energy and centre-of-mass pseudorapidity selection, and is reported in the region $E_T^\gamma > 25$ GeV where reference data is available. Furthermore, the ratio of $R_{p\text{Pb}}$ in the forward region to that in the backward region is presented. The measurements are compared with next-to-leading-order (NLO) pQCD predictions from JETPHOX [23] using parton distribution functions (PDF) extracted from global analyses that include nuclear modification effects analyses [24,25]. Additionally, the data are compared with predictions from a model including initial-state energy loss [4,5,26].

2. Experimental set-up

The ATLAS detector [27] is a multipurpose detector with a forward–backward symmetric cylindrical geometry. For this measurement, its relevant components include an inner tracking detector surrounded by a thin superconducting solenoid, and electromagnetic and hadronic calorimeters. The inner-detector system

is immersed in a 2 T axial magnetic field and provides charged-particle tracking in the pseudorapidity range $|\eta^{\text{lab}}| < 2.5$ in the laboratory frame. In order of closest to furthest from the beam pipe, it consists of a high-granularity silicon pixel detector, a silicon microstrip tracker, and a transition radiation tracker. Additionally, the new insertable B-layer [28] has been operating as the innermost layer of the tracking system since 2015. The calorimeter system covers the range $|\eta^{\text{lab}}| < 4.9$. In the region $|\eta^{\text{lab}}| < 3.2$, electromagnetic calorimetry is provided by barrel and endcap high-granularity lead/liquid-argon (LAr) sampling calorimeters. An additional thin LAr presampler covers $|\eta^{\text{lab}}| < 1.8$ to correct for energy loss in material before the calorimeters. The LAr calorimeters are divided into three layers in radial depth. Hadronic calorimetry is provided by a steel/scintillator-tile calorimeter, segmented into three barrel structures within $|\eta^{\text{lab}}| < 1.7$, and two copper/LAr hadronic endcap calorimeters, which cover the region $1.5 < |\eta^{\text{lab}}| < 3.2$. Finally, the forward calorimeter covers $3.2 < |\eta^{\text{lab}}| < 4.9$ and is divided into three compartments. The first compartment is a copper/LAr electromagnetic calorimeter, while the remaining two tungsten/LAr calorimeter compartments collect the hadronic energy.

During data-taking, events were initially selected using a level-1 trigger, implemented in custom electronics, based on energy deposition in the electromagnetic calorimeter. The high-level trigger [29] was then used to select events consistent with a high- E_T^γ photon candidate. The high level trigger was configured with five online E_T^γ thresholds from 15 GeV to 35 GeV. Each trigger is used for an exclusive region of the E_T^γ spectrum, starting 5 GeV above the trigger threshold because there the trigger is fully efficient. The highest-threshold trigger is used in the measurement over the whole E_T^γ range above 40 GeV and is unrescaled. The lower-threshold, prescaled, triggers are used to perform the measurement for E_T^γ in the range of 20–40 GeV.

Data-taking was divided into two periods with different configurations of the LHC beams. In the first period, the lead ions circulated in beam 1 (clockwise) and protons circulated in beam 2, while in the second period the beams were reversed. These periods corresponded to integrated luminosities of 57 nb^{-1} and 108 nb^{-1} respectively.

3. Photon reconstruction and identification

Photons are reconstructed following a procedure used extensively in previous ATLAS measurements [10], of which only the main features are summarised here.

Photon candidates are reconstructed from clusters of energy deposited in the electromagnetic calorimeter in three regions corresponding to the laboratory-frame (η^{lab}) positions of the barrel and forward and backward endcaps $|\eta^{\text{lab}}| < 2.37$. The transition region between the barrel and endcap calorimeters, $1.37 < |\eta^{\text{lab}}| < 1.56$, is excluded due to its higher level of inactive material. The measurement of the photon energy is based on the energy collected in calorimeter cells in an area of size $\Delta\eta \times \Delta\phi = 0.075 \times 0.175$ in the barrel and $\Delta\eta \times \Delta\phi = 0.125 \times 0.125$ in the endcaps. It is corrected via a dedicated energy calibration [30] which accounts for losses in the material before the calorimeter, both lateral and longitudinal leakage, and for variation of the sampling-fraction with energy and shower depth.

The photons are identified using the tight calorimeter shower shape requirements described in Ref. [31]. The tight requirements select clusters which are compatible with originating from a single photon impacting the calorimeter. The information used includes that from the hadronic calorimeter, the lateral shower shape in the second layer of the electromagnetic calorimeter, and the detailed shower shape in the finely segmented first layer.

¹ ATLAS uses a right-handed coordinate system with its origin at the nominal interaction point (IP) in the centre of the detector and the z-axis along the beam pipe. The x-axis points from the IP to the centre of the LHC ring, and the y-axis points upward. Cylindrical coordinates (r, ϕ) are used in the transverse plane, ϕ being the azimuthal angle around the z-axis. The pseudorapidity is defined in terms of the polar angle θ as $\eta = -\ln \tan(\theta/2)$ and the rapidity of the components of the beam, y , are defined in terms of their energy, E , and longitudinal momentum, p_z , as $y = 0.5 \ln \frac{E+p_z}{E-p_z}$.

The isolation transverse energy, E_T^{iso} , is computed from the sum of E_T values in topological clusters of calorimeter cells [32] inside a cone of size $\Delta R = 0.4$ centred on the photon. This cone size is chosen to be compatible with a previous measurement of photon production in pp collisions at $\sqrt{s} = 8$ TeV [9], which is used to construct the reference spectrum for the $R_{p\text{Pb}}$ measurement. This estimate excludes an area of $\Delta\eta \times \Delta\phi = 0.125 \times 0.175$ centred on the photon, and is corrected for the expected leakage of the photon energy from this region into the isolation cone.

4. Simulated event samples

Samples of Monte Carlo (MC) simulated events were generated to study the detector performance for signal photons. Proton–proton generators were used as the source of events containing photons. To include the effects of the $p + \text{Pb}$ underlying-event environment, these simulated pp events were combined with $p + \text{Pb}$ events from data before reconstruction. In this way, the simulated events contain the effects of the $p + \text{Pb}$ underlying-event identical to those observed in data.

The PYTHIA 8.186 [33] generator was used to generate the nominal set of MC events, with the NNPDF23LO parton distribution function (PDF) set [34] and a set of generator parameters tuned to reproduce minimum-bias pp events with the same collision energy as that in the $p + \text{Pb}$ data (“A14” tune) [35]. A centre-of-mass boost was applied to the generated events to bring them into the same laboratory frame as the data. The generator simulates the direct photon contribution and, through final-state QED radiation in $2 \rightarrow 2$ QCD processes, also includes the fragmentation photon contributions; these components are defined to be signal photons. Events were generated in six exclusive E_T^γ ranges from 17 GeV to 500 GeV.

An additional MC sample was used to assess the sensitivity of the measurement to this choice of generator. The SHERPA 2.2.4 [36] event generator produces fragmentation photons in a different way from PYTHIA and was thus chosen for the comparison. The NNPDF3.0NNLO PDF set [37] was used, and the events were generated in the same kinematic regions as the PYTHIA events. These events were generated with leading-order matrix elements for photon-plus-jet final states with up to three additional partons, which were merged with the SHERPA parton shower. The SHERPA sample produced results consistent with PYTHIA, and, thus, no correction or uncertainty is applied.

The PYTHIA and SHERPA pp events were passed through a full GEANT4 simulation of the ATLAS detector [38,39]. To model the underlying event effects, each simulated event was combined with a minimum-bias $p + \text{Pb}$ data event and the two were reconstructed together as a single event, using the same algorithms as used for the data. These events were split between the two beam configurations in a proportion matched to that in data-taking. The underlying event activity levels, as characterized by the sum of the transverse energy in the outgoing-Pb-beam side of the forward calorimeter ($3.1 < |\eta^{\text{lab}}| < 4.9$), are different in the photon-containing data events from the minimum-bias data events used in the simulation. Thus, the simulated events were weighted on a per-event basis to match the underlying event activity distribution in data. Furthermore, the photon shower shapes and identification efficiency in simulation were adjusted for small differences previously observed between these quantities in data and in GEANT4 simulation [31].

5. Data analysis

The differential cross-section is calculated for each E_T^γ and η^* bin as

$$\frac{d\sigma}{dE_T^\gamma} = \frac{1}{L_{\text{int}}} \frac{1}{\Delta E_T^\gamma} \frac{N_{\text{sig}} P_{\text{sig}}}{\epsilon^{\text{sel}} \epsilon^{\text{trig}}} C_{\text{MC}},$$

where L_{int} is the integrated luminosity, ΔE_T^γ is the width of the E_T^γ bin, N_{sig} is the yield of photon candidates passing identification and isolation requirements, P_{sig} is the purity of the signal selection, ϵ^{sel} is the combined reconstruction, identification and isolation efficiency for signal photons, ϵ^{trig} is the trigger efficiency, and C_{MC} is a MC derived bin-by-bin correction for the change in the E_T^γ spectrum from photons migrating between bins in the spectrum due to the width in the energy response. C_{MC} is determined after all selection criteria at both reconstruction and particle levels are imposed.

Trigger efficiencies ϵ^{trig} are studied using events selected with minimum-bias triggers, level-1 triggers without additional requirements, and photon high-level triggers without identification requirements. They are greater than 99.5% for all triggers [29]. In this analysis they are taken as $\epsilon^{\text{trig}} = 1$, and any uncertainty is neglected as being sub-dominant to other uncertainties.

The purity P_{sig} is determined via a double-sideband procedure used extensively in previous measurements of cross-sections for processes with a photon in the final state [9,10,40,41] and summarised here. In the procedure, four regions are defined which categorise photon candidates along two axes: (1) isolation, corresponding to an isolated and an inverted “non-isolated” selection; (2) identification, corresponding to photons that pass the tight identification requirements described in Ref. [31], and those that pass the loose requirements of Ref. [31] but fail certain components of the tight requirements, designed to mostly select background. The majority of signal photons are in the tight, isolated region, defined to be the signal region, while the other three regions are dominated by the background. Photon candidates that comprise the background are assumed to be distributed in a way that is uncorrelated along the two axes. The yields in the three non-signal sidebands are used to estimate the yield of background in the signal region and is combined with the yield in the signal region to extract the purity. The procedure also accounts for the small fraction of signal photons which are reconstructed in the non-signal sidebands; these quantities, known as leakage fractions, are determined from the simulation samples described in Section 4. The purity is typically 45% at $E_T^\gamma = 20$ GeV, rises to 80% at $E_T^\gamma = 100$ GeV and reaches 99% at $E_T^\gamma = 300$ GeV.

Fig. 1 shows example E_T^{iso} distributions for identified and isolated photons, the corresponding distributions for background photons with the normalisation determined by the double-sideband method, and the resulting signal-photon distributions after background subtraction, compared with those for generator-level photons in MC simulation. The figure shows the shape of the background distribution within the signal region, and the correspondence between the background-subtracted data and the signal-only PYTHIA 8 distributions gives confidence that the simulations accurately represent the data.

The photon selection efficiency is determined from MC simulations. Generated prompt photons are required to be isolated at the generator level, after an estimate of the underlying event has been subtracted from the isolation energy, as described above. Reconstruction efficiency is determined by requiring a photon to have been reconstructed within $\Delta R = 0.2$ of the generated photon. Reconstructed photons matching to a generated photon are further required to satisfy tight identification and isolation criteria defined in Section 1. The combined efficiency of signal photons to pass all reconstruction level selections, ϵ^{sel} , is typically 90% at all E_T^γ and η^* , except at $E_T^\gamma \approx 20$ GeV where it decreases to about 80%. Fig. 2 summarises the different components of the total selection efficiency. The reconstruction efficiency is 96–99% everywhere,

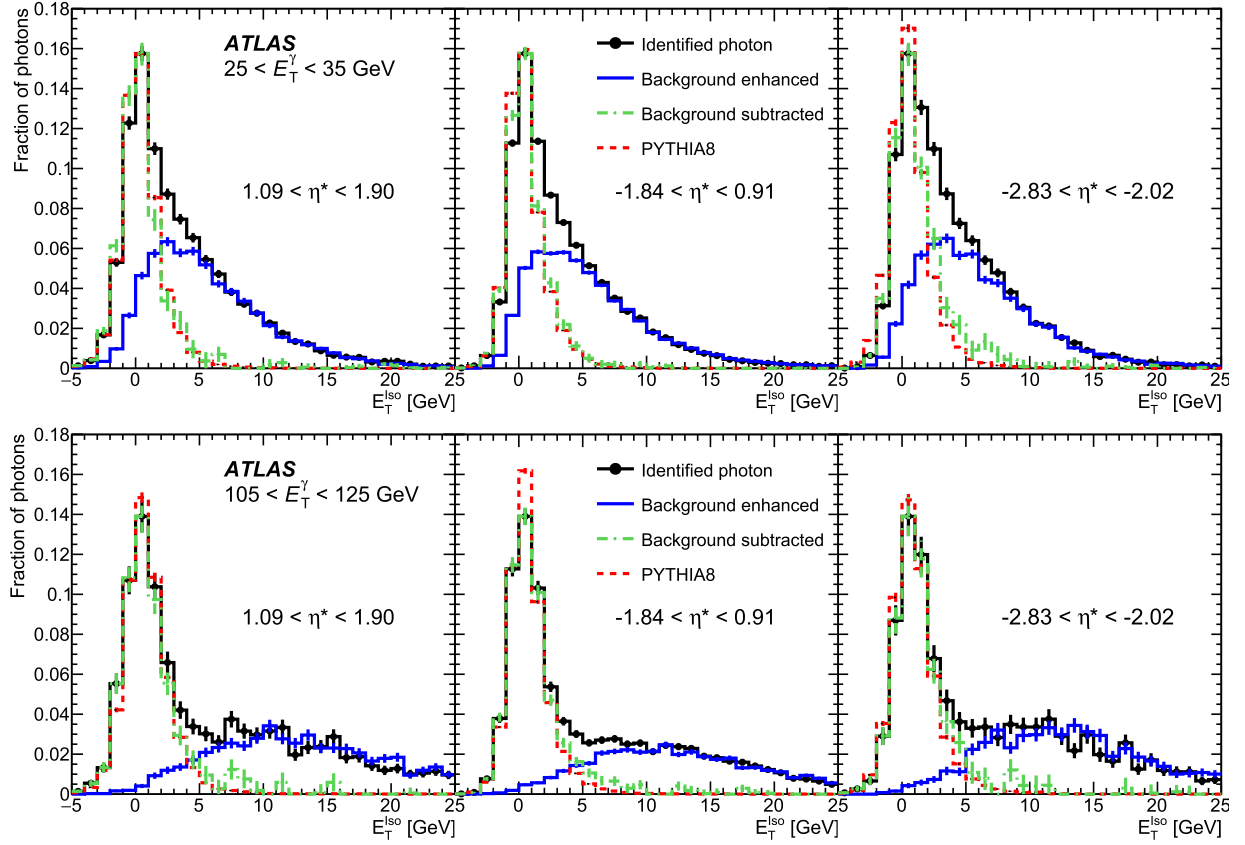


Fig. 1. Distributions of detector-level photon isolation transverse energy E_T^{iso} for identified photons in data (black points), background photons scaled to match the data at large E_T^{iso} (blue solid line), the resulting distribution for signal photons scaled so that the maximum value is the same as that for identified photons (green dot-dashed line), and that for photons in simulation which are isolated at the generator level normalised to have the same integral as the signal photon distribution (red dashed line). Each panel shows a different pseudorapidity region, while the top and bottom panels show the low- E_T^γ and high- E_T^γ range respectively. The vertical error bars represent statistical uncertainties only.

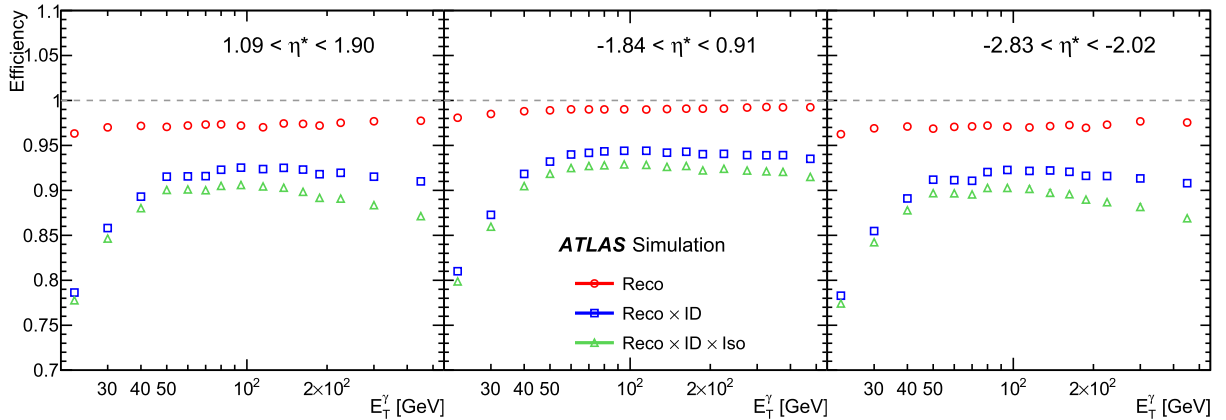


Fig. 2. Efficiency for simulated photons passing the generator-level isolation requirement, shown as a function of photon transverse energy E_T^γ with a different pseudorapidity region in each panel. The reconstruction (red circles), reconstruction plus identification (blue squares) and total selection (green triangles) efficiencies are shown separately.

with the lowest values at the lowest E_T^γ . The isolation efficiency is lowest at high E_T^γ , most likely because the associated products of fragmentation photons are, on average, more energetic and collimated when the energy of the photon is higher. The largest inefficiency is due to the identification requirements. This identification efficiency is lowest at 20 GeV and increases with E_T^γ as higher-energy photons create larger and more identifiable showers in the calorimeter. It peaks around 100 GeV, and decreases with

increasing E_T^γ due to the difficulty of separating conversion electrons at high energy.

In MC events, the E_T response for prompt, isolated photons, defined as the ratio of the reconstructed to generator E_T , is found to be within 1% of unity, with a resolution that decreases from 3% to 2% over the E_T^γ range of the measurement. The bin migration correction factors C_{MC} are determined using the event simulations described in Section 4. They are defined as the bin-by-bin

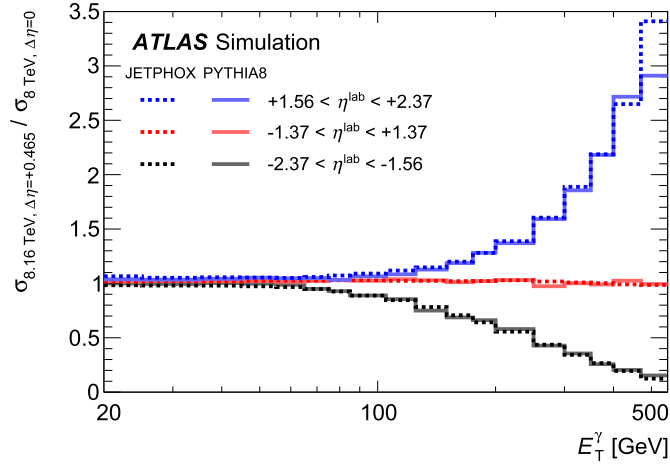


Fig. 3. Summary of extrapolation factors applied to the measured $pp \sqrt{s} = 8$ TeV data to construct an approximate $\sqrt{s} = 8.16$ TeV spectrum matching the shift of the centre-of-mass in $p + \text{Pb}$ data plotted as a function of generator-level photon transverse energy. Here $\Delta\eta$ represents the boost of the centre-of-mass frame of 0.465. The factors determined using JETPHOX (dashed lines) and PYTHIA 8 (solid lines) are shown for the three η^{lab} ranges used in the measurement (different colours). The relative difference between these two extrapolation methods is taken as a systematic uncertainty.

ratio $C_{\text{MC}} = N_{\text{MC}}^{\text{part}} / N_{\text{MC}}^{\text{reco}}$ of the reconstructed, identified, and isolated photon E_T^{γ} spectrum, where $N_{\text{MC}}^{\text{part}}$ is the number in a given E_T^{γ} bin at the particle level and $N_{\text{MC}}^{\text{reco}}$ is the number in the corresponding bin at the reconstruction level.

The nuclear modification factor $R_{p\text{Pb}}$ can be expressed as a ratio of cross-sections in the following way:

$$R_{p\text{Pb}} = (d\sigma^{p+\text{Pb} \rightarrow \gamma+X} / dE_T^{\gamma}) / (A \cdot d\sigma^{pp \rightarrow \gamma+X} / dE_T^{\gamma}), \quad (1)$$

where the geometric factor A is simply the number of nucleons in the Pb nucleus, 208. The reference pp spectrum is constructed using measurements of $\sqrt{s} = 8$ TeV pp data by ATLAS [9] that use the same particle-level isolation requirement. The 8 TeV measurements in the regions $|\eta^{\text{lab}}| < 1.37$ and $1.56 < |\eta^{\text{lab}}| < 2.37$ are used as the reference spectra for the central and the forward and backward rapidity data, after applying a multiplicative correction for the effects of the boost in the 8.16 TeV $p + \text{Pb}$ system. For each kinematic region, extrapolation factors are determined as the ratio of photon cross sections from JETPHOX calculations for pp collisions. The numerator has $\sqrt{s} = 8.16$ TeV with a boost of the centre-of-mass corresponding to the $p + \text{Pb}$ system, and the denominator has en-

ergy $\sqrt{s} = 8$ TeV with its rest frame corresponding with that of the laboratory reference frame. That is, the cross-sections in the numerator and denominator use the same η^{lab} regions, although in the former case this corresponds to a different centre-of-mass pseudorapidity. These factors are shown in Fig. 3 and are applied as multiplicative factors to the measured 8 TeV data. They are dominated by the effect from the boost of the $p + \text{Pb}$ system, as the effect due to the difference in collision energy alone is less than 1% for all E_T^{γ} . For $-1.84 < \eta^* < 0.91$, or $E_T^{\gamma} < 100$ GeV at large rapidities, the factors are typically within a few percent of unity. However, at large E_T^{γ} , where the rapidity distribution becomes steeper, the extrapolation factors become more sensitive to the rapidity shift from the centre-of-mass boost between the frames, and at large pseudorapidity they reach a factor of 2–3. An alternative set of factors, derived from the generator-level predictions of PYTHIA 8, are also shown in Fig. 3; these are used to assess the sensitivity of the extrapolation factors to the rapidity and E_T^{γ} dependence of the model cross sections.

6. Systematic uncertainties

The sources of systematic uncertainties affecting the measurement are described in this section, which is broken into two parts discussing the uncertainty in 1) the cross-section and 2) the nuclear modification factor $R_{p\text{Pb}}$, including its ratio between forward and backward pseudorapidity regions.

6.1. Cross-section uncertainty

The major uncertainties in the cross-section can be divided into two main categories: those affecting the purity determination, which are dominant at low E_T^{γ} where the sample purity is low, and those affecting the detector performance corrections, which are dominant at high E_T^{γ} . All other sources tend to be weakly dependent on E_T^{γ} . A summary is shown in Fig. 4. In each category, the uncertainty is the sum in quadrature of the individual components; the combined uncertainty is the sum in quadrature of all contributions, excluding those associated with the luminosity. The total uncertainties range from 15% at low and high E_T^{γ} , where they are dominated by the purity and detector performance uncertainties respectively, to a minimum of approximately 6% at $E_T^{\gamma} \approx 100$ GeV, where both of these uncertainties are modest.

To assess the uncertainty in the purity determination, each boundary defining the sidebands used in the calculation is varied independently in order to understand the sensitivity of the

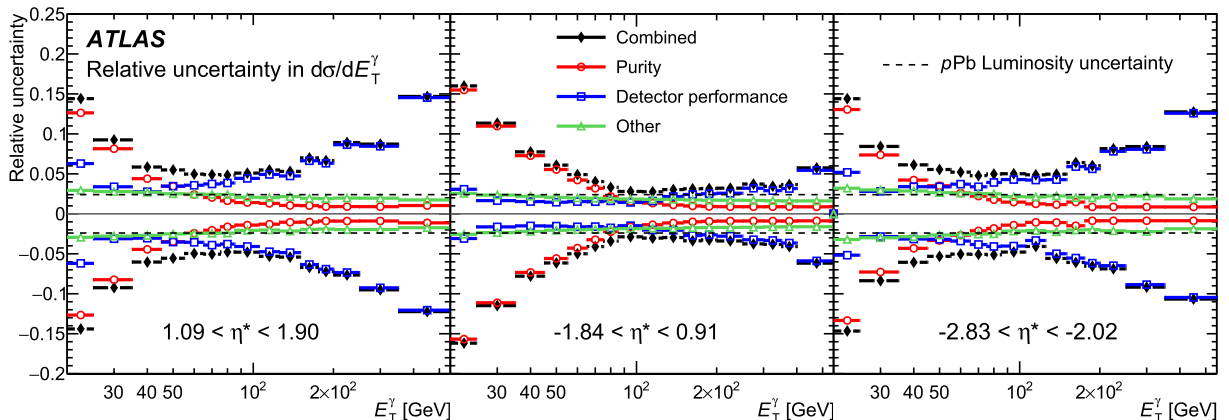


Fig. 4. Summary of the relative sizes of major sources of systematic uncertainty in the cross-section measurement, as well as the combined uncertainty (excluding luminosity), shown as a function of photon transverse energy E_T^{γ} .

measurement to the double sideband binning and correlation assumptions. The dominant uncertainty arises from uncertainty in the level of sideband correlation. This is estimated directly from data by dividing the non-isolated region in two subregions and calculating the ratio of identified to background-enhanced yields in each subregion. These ratios differ at the level of 10% which agrees with estimates from previous studies [10]. This $\pm 10\%$ variation in the sideband correlation yields a 13% uncertainty in the cross-section in the lowest E_T^γ range, decreasing to less than 1% for $E_T^\gamma > 100$ GeV. The inverted photon identification requirement for the background candidates is varied to be less or more restrictive about which shower shapes the background candidates are required to fail. This variation yields an uncertainty that is less than 1% for all E_T^γ in the forward and backward rapidity bins, but is significant at mid-rapidity ($-1.84 < \eta^* < 0.91$) where it is 9% in the lowest E_T^γ bin and decreases to be less than 1% for $E_T^\gamma > 100$ GeV. Variations in the isolation energy threshold of ± 1 GeV have been shown to cover any difference between simulations and data [10]. These variations result in a 1–2% effect on the cross-section in the lowest E_T^γ range and less than 1% at higher E_T^γ . The uncertainty associated with the inverted shower-shape was smoothed and symmetrised, however, the other uncertainties are derived asymmetrically from the positive and negative variations separately.

Uncertainties associated with detector performance corrections are dominant at high E_T^γ . A detailed description of the several components of the photon energy scale and resolution uncertainties are given in Ref. [10]. The impact of these on the measurement is determined by varying the reconstructed photon E_T^γ in simulation within the energy scale uncertainties and deriving alternative correction factors for positive and negative variations separately. Of these, the impact of the energy scale variation is dominant, giving a 10–15% contribution at 500 GeV in the forward and backward regions, decreasing to less than 2% at the lowest E_T^γ . In the mid-rapidity region, the energy scale variation gives a 5% uncertainty at high E_T^γ , decreasing to less than 1% at low E_T^γ . Additionally, there are uncertainties associated with corrections for small differences in reconstruction, identification and isolation efficiencies observed between data and simulation [31]. These uncertainties are about 5% in the forward regions and low E_T^γ and less than 2% elsewhere.

Systematic uncertainties related to modelling in simulation, luminosity, electron contamination, and other sources tend to be lower than those previously discussed. However, their combined effect is dominant in the mid-rapidity region and between 90 GeV and 250 GeV. To test the sensitivity of the measurement to the difference of isolation energy between particle-level and detector level in the simulation, the generator-level isolation definition is changed to better correspond to the reconstruction-level definition. The relative change in the cross-section after this deviation from the nominal is about 2% at low E_T^γ , decreasing to about 1% at high E_T^γ , for each pseudorapidity region, and is taken as a symmetric uncertainty. An uncertainty is assigned to cover the possible contribution of misreconstructed electrons, primarily from the decays of W^\pm and Z bosons, to the selected photon yield. Based on simulation studies, and the results of previous measurements [9,10], this is assigned to be 1.3% for $E_T^\gamma < 105$ GeV in forward pseudorapidity regions, and 0.5% everywhere else. To test the beam orientation dependence, the cross-section is measured using the data from each beam configuration separately. The two measurements agree at the level of 1%, well above the statistical uncertainty for most E_T^γ bins. This difference is taken as a global, symmetric uncertainty in the combined results. To test the sensitivity to the relative fractions of direct and fragmentation photons in the MC samples, the simulation is weighted such that the fraction of direct photons is unity, that is, all photons in the sample are direct. This

reflects a conservative difference compared with the default estimate of this fraction of about 50–80% from the MC samples. This variation gives a relative change in the cross-section of approximately 1% for all kinematic regions, which is taken as a systematic uncertainty. The uncertainty in the integrated luminosity of the combined data sample is 2.4%. It is derived, following a methodology similar to that detailed in Ref. [42], and using the LUCID-2 detector for the baseline luminosity measurements [43], from calibration of the luminosity scale using x-y beam-separation scans.

6.2. R_{pPb} uncertainty

The nuclear modification factor R_{pPb} is affected by systematic uncertainties associated with the $p + Pb$ and pp measurements. The uncertainties in the differential cross-section of the pp reference data are obtained directly from Ref. [9]. Due to differences in photon reconstruction, energy calibration, isolation and identification procedures between the pp and $p + Pb$ datasets, the uncertainties are treated as uncorrelated and added in quadrature.

The uncertainty in the extrapolation of the pp E_T^γ spectrum at 8 TeV is determined by using an alternative method to derive the multiplicative extrapolation factors. Instead of JETPHOX, photon cross-sections for the 8 TeV and rapidity-boosted $\sqrt{s} = 8.16$ TeV kinematics are determined from PYTHIA 8. The extrapolation factors from both JETPHOX and PYTHIA 8 are shown in Fig. 3. Additionally, JETPHOX is run with an alternative PDF set to quantify the impact of a given PDF choice. The differences between the extrapolation factors from these two variations, which are at most a few percent in the kinematic region of the measurement and subdominant with respect to the other uncertainties in the cross-sections, are added in quadrature and used as an estimate of the uncertainty in the extrapolation procedure.

For the measurement of the ratio of R_{pPb} values (Eq. (1)) between the forward and backward pseudorapidity regions, each systematic variation affecting the purity and detector performance corrections is applied to the numerator and denominator in a coherent way, allowing them to partially cancel out in the ratio. All uncertainties in the other categories, except those from electron contamination and the beam direction difference, are treated as correlated. For this reason, they cancel out; notably the $p + Pb$ luminosity and pp cross-section uncertainties cancel out completely. The extrapolation uncertainties are treated as independent and are added in quadrature to the other uncertainties in R_{pPb} .

The resulting uncertainty ranges from about 5% at the lowest E_T^γ , where it is dominated by the uncertainty in the purity, to about 3% at mid- E_T^γ , and again about 5% at high E_T^γ , where it is dominated by uncertainty in the energy scale. A summary of the uncertainties in the forward-to-backward ratio is shown in Fig. 5.

7. Results

Photon production cross-sections are shown in Fig. 6 for photons with $E_T^\gamma > 20$ GeV in three pseudorapidity regions. The measured $d\sigma/dE_T^\gamma$ values decrease by five orders of magnitude over the complete E_T^γ range, which extends out to $E_T^\gamma \approx 500$ GeV for photons at mid-rapidity. In PYTHIA 8, photons in this range typically arise from parton configurations in which the parton in the nucleus has Bjorken scale variable, x_A , in the range $3 \times 10^{-3} \lesssim x_A \lesssim 4 \times 10^{-1}$. In the nuclear modified PDF (nPDF) picture, this range probes the so-called shadowing (suppression for $x_A \lesssim 0.1$), anti-shadowing (enhancement for $0.1 \lesssim x_A \lesssim 0.3$), and EMC (suppression for $0.3 \lesssim x_A \lesssim 0.7$) regions [24].

The data are compared with an NLO pQCD calculation similar to that used in Ref. [3], where the data is similarly underestimated

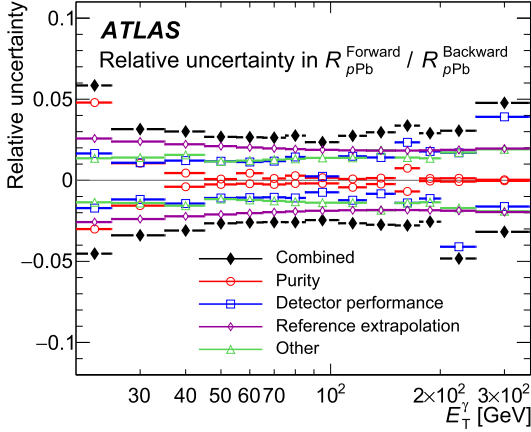


Fig. 5. Summary of the relative size of major sources of systematic uncertainty in the forward-to-backward ratio of the nuclear modification factor R_{pPb} , as well as the combined uncertainty, shown as a function of photon transverse energy E_T^γ . The Reference extrapolation refers to the uncertainty related to the extrapolation of the previously measured 8 TeV pp spectrum to 8.16 TeV and boosted kinematics.

at low E_T , but using the updated CT14 [44] PDF set for the free-nucleon parton densities. JETPHOX [23] is used to perform a full NLO pQCD calculation of the direct and fragmentation contribu-

tions to the cross-section. The BFG set II [45] of parton-to-photon fragmentation functions are used, the number of massless quark flavours is set to five, and the renormalisation, factorisation and fragmentation scales are chosen to be E_T^γ . In addition to the calculation with the free-nucleon PDFs, separate calculations are performed with the EPPS16 [24] and nCTEQ15 [25] nPDF sets. The EPPS16 calculation uses the same free-proton PDF set, CT14, as the free-nucleon baseline to which the modifications are applied. The prediction is systematically lower than the data by up to 20% at low E_T^γ but is closer to the data at higher E_T^γ , consistent with the results of such comparisons in pp collisions at LHC energies [9,10]. A recent calculation of isolated photon production at NNLO found that the predicted cross-sections were systematically larger at low E_T^γ than the NLO prediction [46], and thus may provide a better description of the data in this and previous measurements.

Uncertainties associated with these calculations are assessed in a number of ways. Factorisation, renormalisation, and fragmentation scales are varied, up and down, by a factor of two as in Ref. [9]. The uncertainty is taken as the envelope formed by the minimum and maximum of each variation in every kinematic region and is dominant in most regions. PDF uncertainties are calculated via the standard CT14 error sets and correspond to a 68% confidence interval. Again following Ref. [9] the sensitivity to the choice of α_s is evaluated by varying α_s by ± 0.002 around the central value of 0.118 in the calculation and PDF. Uncertainties from

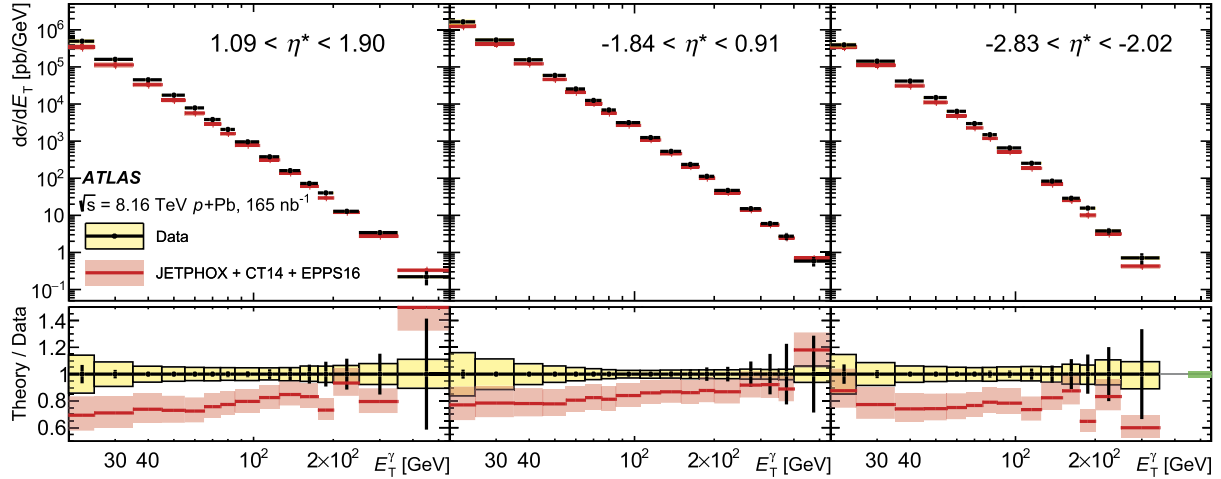


Fig. 6. Prompt, isolated photon cross-sections as a function of transverse energy E_T^γ , shown for different centre-of-mass pseudorapidity, η^* , regions in each panel. The data are compared with JETPHOX with the EPPS16 nuclear PDF set [24], with the ratio of theory to data shown in the lower panels. Yellow bands correspond to total systematic uncertainties in the data (not including the luminosity uncertainty), vertical bars correspond to the statistical uncertainties in the data, and the red bands correspond to the uncertainties in the theoretical calculation. The green box (at the far right) represents the 2.4% luminosity uncertainty.

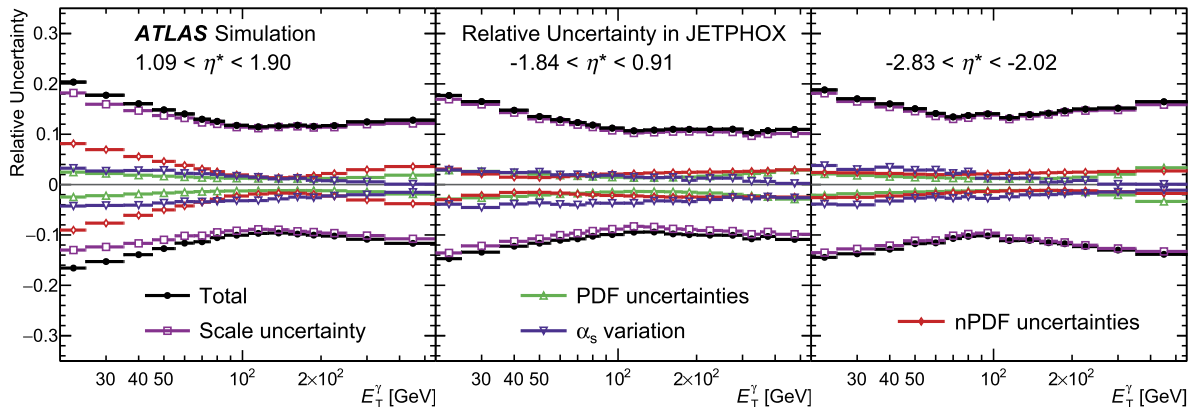


Fig. 7. A breakdown of all systematic uncertainties in the cross-section prediction from JETPHOX with the EPPS16 nPDF set.

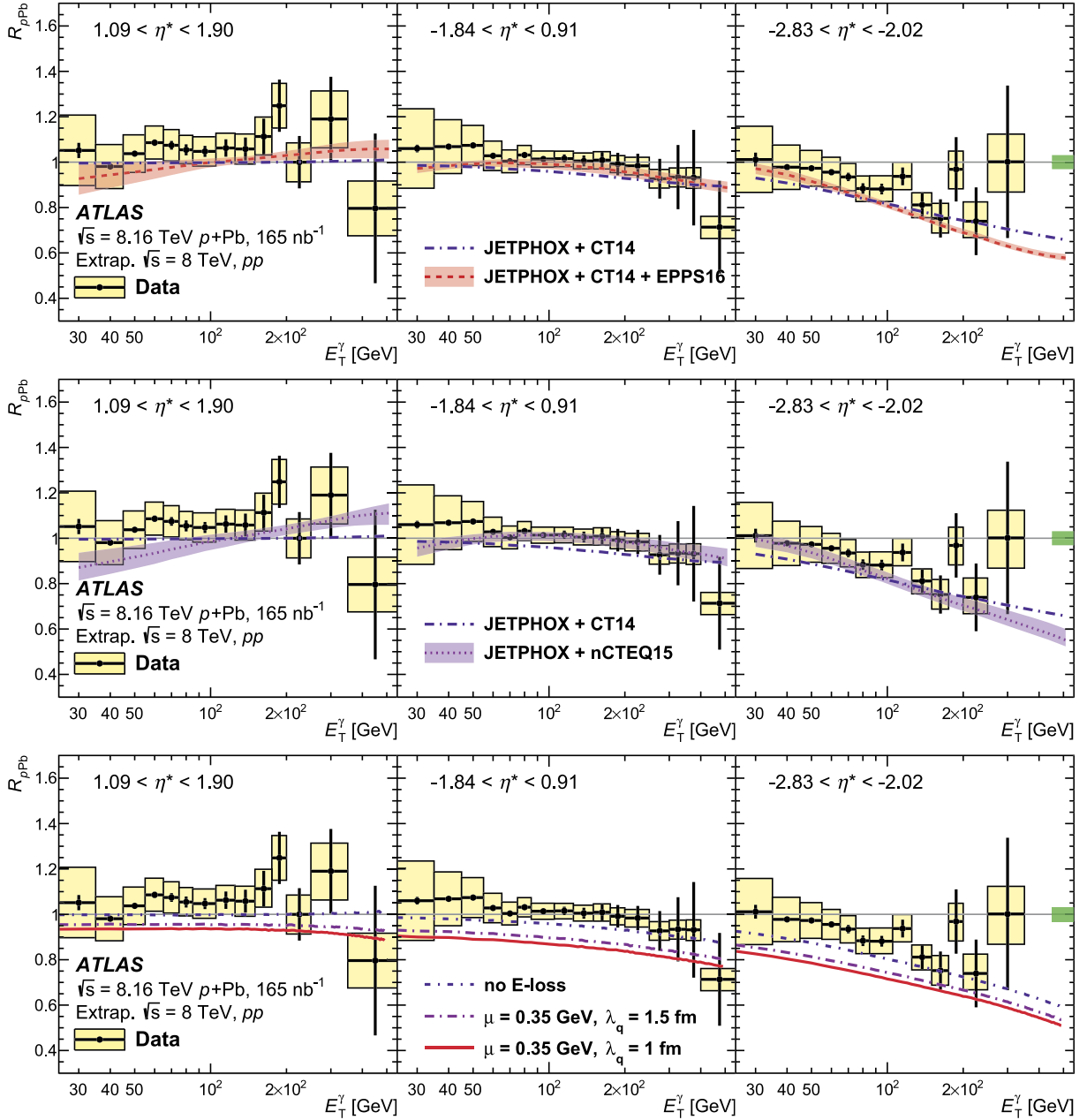


Fig. 8. Nuclear modification factor R_{pPb} for isolated, prompt photons as a function of photon transverse energy E_T^γ , shown for different centre-of-mass pseudorapidity, η^* , regions in each panel. The R_{pPb} is measured using a reference which is a simulation-derived extrapolation from $\sqrt{s} = 8$ TeV pp data (see text). The data are identical in each row, but show comparisons with the expectations based on JETPHOX with the EPPS16 nuclear PDF set (top) [24], with the nCTEQ15 nuclear PDF set (middle) [25], and with an initial-state energy-loss calculation (bottom) [4,5,26]. In all plots, the yellow bands and vertical bars correspond to total systematic and statistical uncertainties in the data respectively. In the top and middle panels, the red and purple bands correspond to the systematic uncertainties in the theoretical calculations. The green box (at the far right) represents the combined 2.4% $p + Pb$ and 1.9% pp luminosity uncertainties.

nPDFs are calculated from the error sets which correspond to 90% confidence intervals, as described in Ref. [24]. These are converted into uncertainty bands which correspond to a 68% confidence interval. A summary of each variation is shown in Fig. 7.

Fig. 8 shows the nuclear modification factor R_{pPb} as a function of E_T^γ in different η^* regions. At forward rapidities ($1.09 < \eta^* < 1.90$), the R_{pPb} value is consistent with unity, indicating that nuclear effects are small. In PYTHIA 8, photons in this region typically arise from configurations with gluon partons from the Pb nucleus with $x_A \approx 10^{-2}$. Nuclear modification pulls the pQCD calculation down slightly for $E_T^\gamma < 100$ GeV, above which the modification reverses, indicating a crossover between shadowing and

anti-shadowing regions. At mid-rapidity, nuclear effects are similarly small and consistent with unity at low E_T^γ , but at higher E_T^γ , there is a hint that R_{pPb} is lower. This feature primarily reflects the different up- and down-quark composition of the nucleus relative to the proton and is more important at larger parton x . In this case, the larger relative down-quark density decreases the photon yield. This effect is evident in the JETPHOX theory curve in blue dash-dotted line, which includes the proton–neutron asymmetry and the free-nucleon PDF set CT14. This effect is most pronounced at backward pseudorapidity where, in PYTHIA 8, the nuclear parton composition is typically a quark with $x_A \approx 0.2$. Here, nPDF modification moves R_{pPb} above the free-nucleon PDF calculation at low

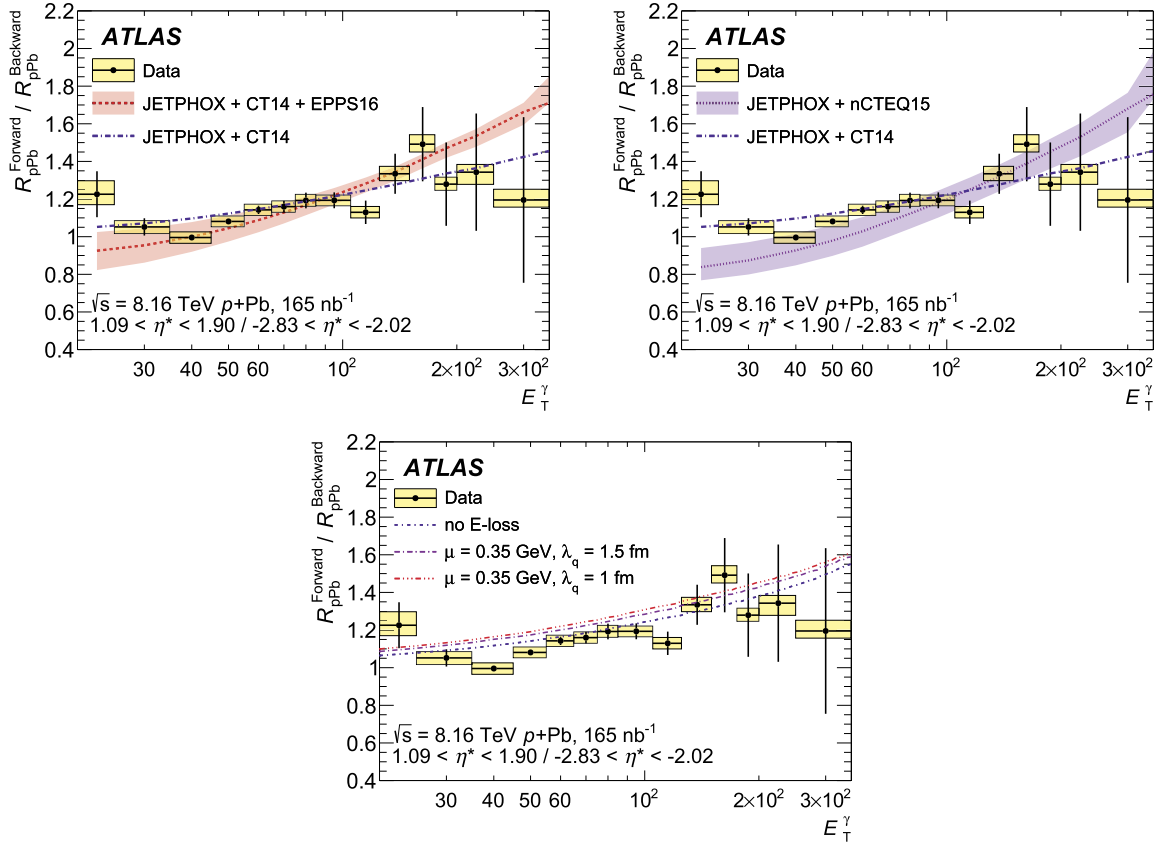


Fig. 9. Ratio of the nuclear modification factor R_{pPb} between forward and backward pseudorapidity for isolated, prompt photons as a function of photon transverse energy E_T^γ . The data are identical in each panel, but show comparisons with the expectations based on JETPHOX with the EPPS16 nuclear PDF set (top, left) [24] or with the nCTEQ15 nuclear PDF set (top, right) [25], and with an initial-state energy-loss calculation (bottom) [4,5,26]. The strength of the initial-state energy-loss effect is parameterised by λ_q , which represents the mean free path of partons in the nuclear medium and is smaller for a larger degree of energy loss. In all plots, the yellow bands and vertical bars correspond to total systematic and statistical uncertainties in the data respectively. In the left and right panels, the red and purple bands correspond to the systematic uncertainties in the calculations.

E_T^γ but below at high E_T^γ , indicating the crossover from the anti-shadowing to the EMC region.

The R_{pPb} calculations including nPDFs consider only the nPDF uncertainty, since previous calculations have shown that the scale and PDF uncertainties cancel out almost completely in the kinematic region of the measurement [3], and no non-perturbative corrections are applied. Within the present uncertainties, the data are consistent with both the free-proton PDFs and with the small effects expected from a nuclear modification of the parton densities.

The R_{pPb} measurements are also compared with an initial-state energy-loss prediction that is calculated within the framework described in Refs. [4,5,24]. In this model, the energetic partons undergo multiple scattering in the cold nuclear medium, and thus lose energy due to this medium-induced gluon bremsstrahlung, before the hard collision. The calculation is performed with a parton-gluon momentum transfer $\mu = 0.35$ GeV and mean free path for quarks $\lambda_q = 1.5$ fm. Alternative calculations with a shorter path length ($\lambda_q = 1$ fm), and a control version with no initial-state energy loss, are also considered. The data disfavour a large suppression of the cross-section from initial-state energy-loss effects.

The ratio of the R_{pPb} values between forward and backward pseudorapidity, shown in Fig. 9, is studied as a way to reduce the effect of common systematic uncertainties and better isolate the magnitude of nuclear effects [47]. The remaining systematic uncertainty, discussed in Sec. 6.2, is dominated by the reference extrapolation and treated as uncorrelated between points. Below

$E_T^\gamma \approx 100$ GeV, this corresponds roughly to the ratio of R_{pPb} from photons from gluon nuclear parton configurations in the shadowing x_A region to that from quark partons in the anti-shadowing region. This can be seen in the top two panels of Fig. 9, where the nuclear modification (red/purple bands) brings the JETPHOX calculation below that of the free-nucleon PDF (blue curve), though the effect from EPPS16 is less significant. In contrast, the behaviour is reversed at higher E_T^γ where the numerator probes the shadowing/anti-shadowing crossover region and the denominator moves deeper into the EMC region [24]. The data are consistent with the pQCD calculation before incorporating nuclear effects, except possibly in the region $E_T^\gamma < 55$ GeV, which is sensitive to the effects from gluon shadowing. At low E_T^γ , the data are systematically higher than the calculations which incorporate nPDF effects, but approximately within their theoretical uncertainty. Additionally, in the lower plot of Fig. 9, the forward-to-backward ratios are compared with predictions from a model incorporating initial-state energy loss. The data show a preference for no or only a limited amount of energy loss.

8. Conclusion

This letter presents a measurement of the inclusive prompt, isolated photon cross-section in $p + \text{Pb}$ collisions at $\sqrt{s_{NN}} = 8.16$ TeV, using a dataset corresponding to an integrated luminosity of 165 nb^{-1} recorded by the ATLAS experiment at the LHC. The differential cross-section as a function of the photon transverse energy is reported in three pseudorapidity regions in the

nucleon–nucleon collision frame, and covers photon transverse energies from 20 GeV to 550 GeV. The data are compared with a next-to-leading-order calculation which incorporates nuclear PDF effects. A measurement of the nuclear modification factor is reported in the region above 25 GeV using a NLO pQCD-based extrapolation of previously published pp data at $\sqrt{s} = 8$ TeV. The data are compatible with the expectation that the PDFs are modestly modified in nuclei in this kinematic region and may help to place an upper limit on the possible amount of energy lost by partons in the initial stages of nuclear collisions.

Acknowledgements

We thank CERN for the very successful operation of the LHC, as well as the support staff from our institutions without whom ATLAS could not be operated efficiently.

We acknowledge the support of ANPCyT, Argentina; YerPhI, Armenia; ARC, Australia; BMWFW and FWF, Austria; ANAS, Azerbaijan; SSTC, Belarus; CNPq and FAPESP, Brazil; NSERC, NRC and CFI, Canada; CERN; CONICYT, Chile; CAS, MOST and NSFC, China; COLCIENCIAS, Colombia; MSMT CR, MPO CR and VSC CR, Czech Republic; DNRF and DNSRC, Denmark; IN2P3-CNRS, CEA-DRF/IRFU, France; SRNSFG, Georgia; BMBF, HGF, and MPG, Germany; GSRT, Greece; RGC, Hong Kong SAR, China; ISF and Benoziyo Center, Israel; INFN, Italy; MEXT and JSPS, Japan; CNRST, Morocco; NWO, Netherlands; RCN, Norway; MNiSW and NCN, Poland; FCT, Portugal; MNE/IFA, Romania; MES of Russia and NRC KI, Russian Federation; JINR; MESTD, Serbia; MSSR, Slovakia; ARRS and MIZŠ, Slovenia; DST/NRF, South Africa; MINECO, Spain; SRC and Wallenberg Foundation, Sweden; SERI, SNSF and Cantons of Bern and Geneva, Switzerland; MOST, Taiwan; TAEK, Turkey; STFC, United Kingdom; DOE and NSF, United States of America. In addition, individual groups and members have received support from BCKDF, Canarie, CRC and Compute Canada, Canada; COST, ERC, ERDF, Horizon 2020, and Marie Skłodowska-Curie Actions, European Union; Investissements d’Avenir Labex and Idex, ANR, France; DFG and AvH Foundation, Germany; Herakleitos, Thales and Aristeia programmes co-financed by EU-ESF and the Greek NSRF, Greece; BSF-NSF and GIF, Israel; CERCA Programme Generalitat de Catalunya, Spain; The Royal Society and Leverhulme Trust, United Kingdom.

The crucial computing support from all WLCG partners is acknowledged gratefully, in particular from CERN, the ATLAS Tier-1 facilities at TRIUMF (Canada), NDGF (Denmark, Norway, Sweden), CC-IN2P3 (France), KIT/GridKA (Germany), INFN-CNAF (Italy), NL-T1 (Netherlands), PIC (Spain), ASGC (Taiwan), RAL (UK) and BNL (USA), the Tier-2 facilities worldwide and large non-WLCG resource providers. Major contributors of computing resources are listed in Ref. [48].

References

- [1] C.A. Salgado, et al., Proton-nucleus collisions at the LHC: scientific opportunities and requirements, *J. Phys. G* 39 (2012) 015010, arXiv:1105.3919 [hep-ph] (cit. on p. 2).
- [2] F. Arleo, K.J. Eskola, H. Paukkunen, C.A. Salgado, Inclusive prompt photon production in nuclear collisions at RHIC and LHC, *J. High Energy Phys.* 04 (2011) 055, arXiv:1103.1471 [hep-ph] (cit. on p. 2).
- [3] I. Helenius, K.J. Eskola, H. Paukkunen, Probing the small- x nuclear gluon distributions with isolated photons at forward rapidities in $p + \text{Pb}$ collisions at the LHC, *J. High Energy Phys.* 09 (2014) 138, arXiv:1406.1689 [hep-ph] (cit. on pp. 2, 11, 13).
- [4] I. Vitev, B.-W. Zhang, A systematic study of direct photon production in heavy ion collisions, *Phys. Lett. B* 669 (2008) 337, arXiv:0804.3805 [hep-ph] (cit. on pp. 2, 3, 14, 15).
- [5] Z.-B. Kang, I. Vitev, H. Xing, Effects of cold nuclear matter energy loss on inclusive jet production in $p + A$ collisions at energies available at the BNL Relativistic Heavy Ion Collider and the CERN Large Hadron Collider, *Phys. Rev. C* 92 (2015) 054911, arXiv:1507.05987 [hep-ph] (cit. on pp. 2, 3, 14, 15).
- [6] ATLAS Collaboration, Measurements of the nuclear modification factor for jets in $\text{Pb} + \text{Pb}$ collisions at $\sqrt{s_{\text{NN}}} = 2.76$ TeV with the ATLAS detector, *Phys. Rev. Lett.* 114 (2015) 072302, arXiv:1411.2357 [hep-ex] (cit. on p. 2).
- [7] ATLAS Collaboration, Measurement of charged-particle spectra in $\text{Pb} + \text{Pb}$ collisions at $\sqrt{s_{\text{NN}}} = 2.76$ TeV with the ATLAS detector at the LHC, *J. High Energy Phys.* 09 (2015) 050, arXiv:1504.04337 [hep-ex] (cit. on p. 2).
- [8] ATLAS Collaboration, Measurement of the inclusive isolated prompt photon cross section in pp collisions at $\sqrt{s} = 7$ TeV with the ATLAS detector, *Phys. Rev. D* 83 (2011) 052005, arXiv:1012.4389 [hep-ex] (cit. on p. 2).
- [9] ATLAS Collaboration, Measurement of the inclusive isolated prompt photon cross section in pp collisions at $\sqrt{s} = 8$ TeV with the ATLAS detector, *J. High Energy Phys.* 08 (2016) 005, arXiv:1605.03495 [hep-ex] (cit. on pp. 2–4, 6, 7, 10–12).
- [10] ATLAS Collaboration, Measurement of the cross section for inclusive isolated-photon production in pp collisions at $\sqrt{s} = 13$ TeV using the ATLAS detector, *Phys. Lett. B* 770 (2017) 473, arXiv:1701.06882 [hep-ex] (cit. on pp. 2–4, 6, 9, 10, 12).
- [11] CMS Collaboration, Measurement of the differential cross section for isolated prompt photon production in pp collisions at 7 TeV, *Phys. Rev. D* 84 (2011) 052011, arXiv:1108.2044 [hep-ex] (cit. on p. 2).
- [12] CMS Collaboration, Measurement of the production cross section for pairs of isolated photons in pp collisions at $\sqrt{s} = 7$ TeV, *J. High Energy Phys.* 01 (2012) 133, arXiv:1110.6461 [hep-ex] (cit. on p. 2).
- [13] ATLAS Collaboration, Centrality, rapidity and transverse momentum dependence of isolated prompt photon production in lead–lead collisions at $\sqrt{s_{\text{NN}}} = 2.76$ TeV measured with the ATLAS detector, *Phys. Rev. C* 93 (2016) 034914, arXiv:1506.08552 [hep-ex] (cit. on p. 2).
- [14] ALICE Collaboration, Direct photon production in $\text{Pb}+\text{Pb}$ collisions at $\sqrt{s_{\text{NN}}} = 2.76$ TeV, *Phys. Lett. B* 754 (2016) 235, arXiv:1509.07324 [nucl-ex] (cit. on p. 2).
- [15] PHENIX Collaboration, Measurement of direct photons in $\text{Au} + \text{Au}$ collisions at $\sqrt{s_{\text{NN}}} = 200$ GeV, *Phys. Rev. Lett.* 109 (2012) 152302, arXiv:1205.5759 [nucl-ex] (cit. on p. 2).
- [16] STAR Collaboration, Inclusive π^0 , η , and direct photon production at high transverse momentum in $p + p$ and $d + \text{Au}$ collisions at $\sqrt{s_{\text{NN}}} = 200$ GeV, *Phys. Rev. C* 81 (2010) 064904, arXiv:0912.3838 [hep-ex] (cit. on p. 2).
- [17] PHENIX Collaboration, Direct photon production in $d + \text{Au}$ collisions at $\sqrt{s_{\text{NN}}} = 200$ GeV, *Phys. Rev. C* 87 (2013) 054907, arXiv:1208.1234 [nucl-ex] (cit. on p. 2).
- [18] ATLAS Collaboration, Centrality and rapidity dependence of inclusive jet production in $\sqrt{s_{\text{NN}}} = 5.02$ TeV proton–lead collisions with the ATLAS detector, *Phys. Lett. B* 748 (2015) 392, arXiv:1412.4092 [hep-ex] (cit. on p. 2).
- [19] CMS Collaboration, Measurement of inclusive jet production and nuclear modifications in $p\text{Pb}$ collisions at $\sqrt{s_{\text{NN}}} = 5.02$ TeV, *Eur. Phys. J. C* 76 (2016) 372, arXiv:1601.02001 [hep-ex] (cit. on p. 2).
- [20] ATLAS Collaboration, Z boson production in $p + \text{Pb}$ collisions at $\sqrt{s_{\text{NN}}} = 5.02$ TeV measured with the ATLAS detector, *Phys. Rev. C* 92 (2015) 044915, arXiv:1507.06232 [hep-ex] (cit. on p. 2).
- [21] CMS Collaboration, Study of Z boson production in $p\text{Pb}$ collisions at $\sqrt{s_{\text{NN}}} = 5.02$ TeV, *Phys. Lett. B* 759 (2016) 36, arXiv:1512.06461 [hep-ex] (cit. on p. 2).
- [22] CMS Collaboration, Study of W boson production in $p\text{Pb}$ collisions at $\sqrt{s_{\text{NN}}} = 5.02$ TeV, *Phys. Lett. B* 750 (2015) 565, arXiv:1503.05825 [hep-ex] (cit. on p. 2).
- [23] P. Aurenche, M. Fontannaz, J.-P. Guillet, E. Pilon, M. Werlen, Recent critical study of photon production in hadronic collisions, *Phys. Rev. D* 73 (2006) 094007, arXiv:hep-ph/0602133 [hep-ph] (cit. on pp. 3, 11).
- [24] K.J. Eskola, P. Paakkinen, H. Paukkunen, C.A. Salgado, EPPS16: nuclear parton distributions with LHC data, *Eur. Phys. J. C* 77 (2017) 163, arXiv:1612.05741 [hep-ph] (cit. on pp. 3, 11–16).
- [25] K. Kovarik, et al., nCTEQ15 – global analysis of nuclear parton distributions with uncertainties in the CTEQ framework, *Phys. Rev. D* 93 (2016) 085037, arXiv:1509.00792 [hep-ph] (cit. on pp. 3, 11, 14, 15).
- [26] Y.-T. Chien, A. Emerman, Z.-B. Kang, G. Ovanessian, I. Vitev, Jet quenching from QCD evolution, *Phys. Rev. D* 93 (2016) 074030, arXiv:1509.02936 [hep-ph] (cit. on pp. 3, 14, 15).
- [27] ATLAS Collaboration, The ATLAS experiment at the CERN Large Hadron Collider, *J. Instr.* 3 (2008) S08003 (cit. on p. 3).
- [28] ATLAS Collaboration, ATLAS Insertable B-Layer Technical Design Report, ATLAS-TDR-19, 2010, <https://cds.cern.ch/record/1291633>, ATLAS Insertable B-Layer Technical Design Report Addendum, ATLAS-TDR-19-ADD-1, <https://cds.cern.ch/record/1451888>, 2012 (cit. on p. 3).
- [29] ATLAS Collaboration, Performance of the ATLAS trigger system in 2015, *Eur. Phys. J. C* 77 (2017) 317, arXiv:1611.09661 [hep-ex] (cit. on pp. 4, 6).
- [30] ATLAS Collaboration, Electron and photon energy calibration with the ATLAS detector using 2015–2016 LHC proton–proton collision data, arXiv:1812.03848 [hep-ex], 2018 (cit. on p. 4).
- [31] ATLAS Collaboration, Measurement of the photon identification efficiencies with the ATLAS detector using LHC Run 2 data collected in 2015 and 2016, *Eur. Phys. J.* (2018), arXiv:1810.05087 [hep-ex] (cit. on pp. 4–6, 10).

- [32] ATLAS Collaboration, Topological cell clustering in the ATLAS calorimeters and its performance in LHC Run 1, *Eur. Phys. J. C* 77 (2017) 490, arXiv:1603.02934 [hep-ex] (cit. on p. 4).
- [33] T. Sjöstrand, S. Mrenna, P.Z. Skands, A brief introduction to PYTHIA 8.1, *Comput. Phys. Commun.* 178 (2008) 852, arXiv:0710.3820 [hep-ph] (cit. on p. 5).
- [34] R.D. Ball, et al., Parton distributions with LHC data, *Nucl. Phys. B* 867 (2013) 244, arXiv:1207.1303 [hep-ph] (cit. on p. 5).
- [35] ATLAS Collaboration, ATLAS Pythia 8 Tunes to 7 TeV Data, ATL-PHYS-PUB-2014-021, <https://cds.cern.ch/record/1966419>, 2014 (cit. on p. 5).
- [36] T. Gleisberg, et al., Event generation with SHERPA 1.1, *J. High Energy Phys.* 02 (2009) 007, arXiv:0811.4622 [hep-ph] (cit. on p. 5).
- [37] R.D. Ball, et al., Parton distributions for the LHC Run II, *J. High Energy Phys.* 04 (2015) 040, arXiv:1410.8849 [hep-ph] (cit. on p. 5).
- [38] S. Agostinelli, et al., GEANT4 – a simulation toolkit, *Nucl. Instrum. Methods A* 506 (2003) 250 (cit. on p. 5).
- [39] ATLAS Collaboration, The ATLAS simulation infrastructure, *Eur. Phys. J. C* 70 (2010) 823, arXiv:1005.4568 [physics.ins-det] (cit. on p. 5).
- [40] ATLAS Collaboration, Measurement of the inclusive isolated prompt photons cross section in pp collisions at $\sqrt{s} = 7$ TeV with the ATLAS detector using 4.6 fb⁻¹, *Phys. Rev. D* 89 (2014) 052004, arXiv:1311.1440 [hep-ex] (cit. on p. 6).
- [41] ATLAS Collaboration, High- E_T isolated-photon plus jets production in pp collisions at $\sqrt{s} = 8$ TeV with the ATLAS detector, *Nucl. Phys. B* 918 (2017) 257, arXiv:1611.06586 [hep-ex] (cit. on p. 6).
- [42] ATLAS Collaboration, Luminosity determination in pp collisions at $\sqrt{s} = 8$ TeV using the ATLAS detector at the LHC, *Eur. Phys. J. C* 76 (2016) 653, arXiv:1608.03953 [hep-ex] (cit. on p. 10).
- [43] G. Avoni, et al., The new LUCID-2 detector for luminosity measurement and monitoring in ATLAS, *J. Instrum.* 13 (2018) P07017 (cit. on p. 10).
- [44] S. Dulat, et al., New parton distribution functions from a global analysis of quantum chromodynamics, *Phys. Rev. D* 93 (2016) 033006, arXiv:1506.07443 [hep-ph] (cit. on p. 11).
- [45] L. Bourhis, M. Fontannaz, J.P. Guillet, Quarks and gluon fragmentation functions into photons, *Eur. Phys. J. C* 2 (1998) 529, arXiv:hep-ph/9704447 [hep-ph] (cit. on p. 11).
- [46] X. Chen, T. Gehrmann, N. Glover, M. Höfer, A. Huss, Isolated photon and photon+jet production at NNLO QCD accuracy, submitted to *J. High Energy Phys.* (2019), arXiv:1904.01044 [hep-ph] (cit. on p. 12), in press.
- [47] H. Paukkunen, C.A. Salgado, Constraints for the nuclear parton distributions from Z and W production at the LHC, *J. High Energy Phys.* 03 (2011) 071, arXiv:1010.5392 [hep-ph] (cit. on p. 15).
- [48] ATLAS Collaboration, ATLAS Computing Acknowledgements, ATL-GEN-PUB-2016-002, <https://cds.cern.ch/record/2202407> (cit. on p. 17).

The ATLAS Collaboration

M. Aaboud^{34d}, G. Aad⁹⁹, B. Abbott¹²⁵, D.C. Abbott¹⁰⁰, O. Abdinov^{13,*}, B. Abeloos¹²⁹, D.K. Abhayasinghe⁹¹, S.H. Abidi¹⁶⁴, O.S. AbouZeid³⁹, N.L. Abraham¹⁵³, H. Abramowicz¹⁵⁸, H. Abreu¹⁵⁷, Y. Abulaiti⁶, B.S. Acharya^{64a,64b,o}, S. Adachi¹⁶⁰, L. Adam⁹⁷, L. Adamczyk^{81a}, L. Adamek¹⁶⁴, J. Adelman¹¹⁹, M. Adersberger¹¹², A. Adiguzel^{12c,ah}, T. Adye¹⁴¹, A.A. Affolder¹⁴³, Y. Afik¹⁵⁷, C. Agheorghiesei^{28c}, J.A. Aguilar-Saavedra^{137f,137a,ag}, F. Ahmadov^{77,ae}, G. Aielli^{71a,71b}, S. Akatsuka⁸³, T.P.A. Åkesson⁹⁴, E. Akilli⁵², A.V. Akimov¹⁰⁸, G.L. Alberghi^{23b,23a}, J. Albert¹⁷³, P. Albicocco⁴⁹, M.J. Alconada Verzini⁸⁶, S. Alderweireldt¹¹⁷, M. Aleksa³⁵, I.N. Aleksandrov⁷⁷, C. Alexa^{28b}, D. Alexandre¹⁹, T. Alexopoulos¹⁰, M. Alhroob¹²⁵, B. Ali¹³⁹, G. Alimonti^{66a}, J. Alison³⁶, S.P. Alkire¹⁴⁵, C. Allaire¹²⁹, B.M.M. Allbrooke¹⁵³, B.W. Allen¹²⁸, P.P. Allport²¹, A. Aloisio^{67a,67b}, A. Alonso³⁹, F. Alonso⁸⁶, C. Alpigiani¹⁴⁵, A.A. Alshehri⁵⁵, M.I. Alstady⁹⁹, B. Alvarez Gonzalez³⁵, D. Álvarez Piqueras¹⁷¹, M.G. Alviggi^{67a,67b}, B.T. Amadio¹⁸, Y. Amaral Coutinho^{78b}, A. Ambler¹⁰¹, L. Ambroz¹³², C. Amelung²⁷, D. Amidei¹⁰³, S.P. Amor Dos Santos^{137a,137c}, S. Amoroso⁴⁴, C.S. Amrouche⁵², F. An⁷⁶, C. Anastopoulos¹⁴⁶, L.S. Ancu⁵², N. Andari¹⁴², T. Andeen¹¹, C.F. Anders^{59b}, J.K. Anders²⁰, A. Andreazza^{66a,66b}, V. Andrei^{59a}, C.R. Anelli¹⁷³, S. Angelidakis³⁷, I. Angelozzi¹¹⁸, A. Angerami³⁸, A.V. Anisenkov^{120b,120a}, A. Annovi^{69a}, C. Antel^{59a}, M.T. Anthony¹⁴⁶, M. Antonelli⁴⁹, D.J.A. Antrim¹⁶⁸, F. Anulli^{70a}, M. Aoki⁷⁹, J.A. Aparisi Pozo¹⁷¹, L. Aperio Bella³⁵, G. Arabidze¹⁰⁴, J.P. Araque^{137a}, V. Araujo Ferraz^{78b}, R. Araujo Pereira^{78b}, A.T.H. Arce⁴⁷, R.E. Ardell⁹¹, F.A. Arduh⁸⁶, J.-F. Arguin¹⁰⁷, S. Argyropoulos⁷⁵, J.-H. Arling⁴⁴, A.J. Armbruster³⁵, L.J. Armitage⁹⁰, A. Armstrong¹⁶⁸, O. Arnaez¹⁶⁴, H. Arnold¹¹⁸, M. Arratia³¹, O. Arslan²⁴, A. Artamonov^{109,*}, G. Artoni¹³², S. Artz⁹⁷, S. Asai¹⁶⁰, N. Asbah⁵⁷, E.M. Asimakopoulou¹⁶⁹, L. Asquith¹⁵³, K. Assamagan^{26b}, R. Astalos^{29a}, R.J. Atkin^{32a}, M. Atkinson¹⁷⁰, N.B. Atlay¹⁴⁸, K. Augsten¹³⁹, G. Avolio³⁵, R. Avramidou^{58a}, M.K. Ayoub^{15a}, A.M. Azoulay^{165b}, G. Azuelos^{107,av}, A.E. Baas^{59a}, M.J. Baca²¹, H. Bachacou¹⁴², K. Bachas^{65a,65b}, M. Backes¹³², P. Bagnaia^{70a,70b}, M. Bahmani⁸², H. Bahrasemani¹⁴⁹, A.J. Bailey¹⁷¹, V.R. Bailey¹⁷⁰, J.T. Baines¹⁴¹, M. Bajic³⁹, C. Bakalis¹⁰, O.K. Baker¹⁸⁰, P.J. Bakker¹¹⁸, D. Bakshi Gupta⁸, S. Balaji¹⁵⁴, E.M. Baldin^{120b,120a}, P. Balek¹⁷⁷, F. Balli¹⁴², W.K. Balunas¹³⁴, J. Balz⁹⁷, E. Banas⁸², A. Bandyopadhyay²⁴, S. Banerjee^{178,k}, A.A.E. Bannoura¹⁷⁹, L. Barak¹⁵⁸, W.M. Barbe³⁷, E.L. Barberio¹⁰², D. Barberis^{53b,53a}, M. Barbero⁹⁹, T. Barillari¹¹³, M.-S. Barisits³⁵, J. Barkeloo¹²⁸, T. Barklow¹⁵⁰, R. Barnea¹⁵⁷, S.L. Barnes^{58c}, B.M. Barnett¹⁴¹, R.M. Barnett¹⁸, Z. Barnovska-Blenessy^{58a}, A. Baroncelli^{72a}, G. Barone^{26b}, A.J. Barr¹³², L. Barranco Navarro¹⁷¹, F. Barreiro⁹⁶, J. Barreiro Guimarães da Costa^{15a}, R. Bartoldus¹⁵⁰, A.E. Barton⁸⁷, P. Bartos^{29a}, A. Basalae¹³⁵, A. Bassalat¹²⁹, R.L. Bates⁵⁵, S.J. Batista¹⁶⁴, S. Batlamous^{34e}, J.R. Batley³¹, M. Battaglia¹⁴³, M. Bause^{70a,70b}, F. Bauer¹⁴², K.T. Bauer¹⁶⁸, H.S. Bawa¹⁵⁰, J.B. Beacham¹²³, T. Beau¹³³, P.H. Beauchemin¹⁶⁷, P. Bechtel²⁴, H.C. Beck⁵¹, H.P. Beck^{20,r}, K. Becker⁵⁰, M. Becker⁹⁷, C. Becot⁴⁴, A. Beddall^{12d}, A.J. Beddall^{12a}, V.A. Bednyakov⁷⁷, M. Bedognetti¹¹⁸, C.P. Bee¹⁵², T.A. Beermann⁷⁴, M. Begalli^{78b}, M. Begel^{26b}, A. Behera¹⁵², J.K. Behr⁴⁴, F. Beisiegel²⁴, A.S. Bell⁹², G. Bella¹⁵⁸, L. Bellagamba^{23b}, A. Bellerive³³, M. Bellomo¹⁵⁷, P. Bellos⁹, K. Belotskiy¹¹⁰, N.L. Belyaev¹¹⁰,

O. Benary^{158,*}, D. Benchekroun^{34a}, M. Bender¹¹², N. Benekos¹⁰, Y. Benhammou¹⁵⁸,
 E. Benhar Noccioli¹⁸⁰, J. Benitez⁷⁵, D.P. Benjamin⁶, M. Benoit⁵², J.R. Bensinger²⁷, S. Bentvelsen¹¹⁸,
 L. Beresford¹³², M. Beretta⁴⁹, D. Berge⁴⁴, E. Bergeaas Kuutmann¹⁶⁹, N. Berger⁵, B. Bergmann¹³⁹,
 L.J. Bergsten²⁷, J. Beringer¹⁸, S. Berlendis⁷, N.R. Bernard¹⁰⁰, G. Bernardi¹³³, C. Bernius¹⁵⁰,
 F.U. Bernlochner²⁴, T. Berry⁹¹, P. Berta⁹⁷, C. Bertella^{15a}, G. Bertoli^{43a,43b}, I.A. Bertram⁸⁷, G.J. Besjes³⁹,
 O. Bessidskaia Bylund¹⁷⁹, M. Bessner⁴⁴, N. Besson¹⁴², A. Bethani⁹⁸, S. Bethke¹¹³, A. Betti²⁴,
 A.J. Bevan⁹⁰, J. Beyer¹¹³, R. Bi¹³⁶, R.M. Bianchi¹³⁶, O. Biebel¹¹², D. Biedermann¹⁹, R. Bielski³⁵,
 K. Bierwagen⁹⁷, N.V. Biesuz^{69a,69b}, M. Biglietti^{72a}, T.R.V. Billoud¹⁰⁷, M. Bindi⁵¹, A. Bingul^{12d},
 C. Bini^{70a,70b}, S. Biondi^{23b,23a}, M. Birman¹⁷⁷, T. Bisanz⁵¹, J.P. Biswal¹⁵⁸, C. Bittrich⁴⁶, D.M. Bjergaard⁴⁷,
 J.E. Black¹⁵⁰, K.M. Black²⁵, T. Blazek^{29a}, I. Bloch⁴⁴, C. Blocker²⁷, A. Blue⁵⁵, U. Blumenschein⁹⁰,
 Dr. Blunier^{144a}, G.J. Bobbink¹¹⁸, V.S. Bobrovnikov^{120b,120a}, S.S. Bocchetta⁹⁴, A. Bocci⁴⁷, D. Boerner¹⁷⁹,
 D. Bogavac¹¹², A.G. Bogdanchikov^{120b,120a}, C. Bohm^{43a}, V. Boisvert⁹¹, P. Bokan^{51,169}, T. Bold^{81a},
 A.S. Boldyrev¹¹¹, A.E. Bolz^{59b}, M. Bomben¹³³, M. Bona⁹⁰, J.S. Bonilla¹²⁸, M. Boonekamp¹⁴²,
 H.M. Borecka-Bielska⁸⁸, A. Borisov¹²¹, G. Borissov⁸⁷, J. Bortfeldt³⁵, D. Bortoletto¹³², V. Bortolotto^{71a,71b},
 D. Boscherini^{23b}, M. Bosman¹⁴, J.D. Bossio Sola³⁰, K. Bouaouda^{34a}, J. Boudreau¹³⁶,
 E.V. Bouhova-Thacker⁸⁷, D. Boumediene³⁷, C. Bourdarios¹²⁹, S.K. Boutle⁵⁵, A. Boveia¹²³, J. Boyd³⁵,
 D. Boye^{32b,ap}, I.R. Boyko⁷⁷, A.J. Bozson⁹¹, J. Bracinik²¹, N. Brahimi⁹⁹, A. Brandt⁸, G. Brandt¹⁷⁹,
 O. Brandt^{59a}, F. Braren⁴⁴, U. Bratzler¹⁶¹, B. Brau¹⁰⁰, J.E. Brau¹²⁸, W.D. Breaden Madden⁵⁵,
 K. Brendlinger⁴⁴, L. Brenner⁴⁴, R. Brenner¹⁶⁹, S. Bressler¹⁷⁷, B. Brickwedde⁹⁷, D.L. Briglin²¹,
 D. Britton⁵⁵, D. Britzger¹¹³, I. Brock²⁴, R. Brock¹⁰⁴, G. Brooijmans³⁸, T. Brooks⁹¹, W.K. Brooks^{144b},
 E. Brost¹¹⁹, J.H. Broughton²¹, P.A. Bruckman de Renstrom⁸², D. Bruncko^{29b}, A. Bruni^{23b}, G. Bruni^{23b},
 L.S. Bruni¹¹⁸, S. Bruno^{71a,71b}, B.H. Brunt³¹, M. Bruschi^{23b}, N. Bruscino¹³⁶, P. Bryant³⁶, L. Bryngemark⁹⁴,
 T. Buanes¹⁷, Q. Buat³⁵, P. Buchholz¹⁴⁸, A.G. Buckley⁵⁵, I.A. Budagov⁷⁷, M.K. Bugge¹³¹, F. Bühner⁵⁰,
 O. Bulekov¹¹⁰, D. Bullock⁸, T.J. Burch¹¹⁹, S. Burdin⁸⁸, C.D. Burgard¹¹⁸, A.M. Burger⁵, B. Burghgrave⁸,
 K. Burka⁸², S. Burke¹⁴¹, I. Burmeister⁴⁵, J.T.P. Burr¹³², V. Büscher⁹⁷, E. Buschmann⁵¹, P. Bussey⁵⁵,
 J.M. Butler²⁵, C.M. Buttar⁵⁵, J.M. Butterworth⁹², P. Butti³⁵, W. Buttinger³⁵, A. Buzatu¹⁵⁵,
 A.R. Buzykaev^{120b,120a}, G. Cabras^{23b,23a}, S. Cabrera Urbán¹⁷¹, D. Caforio¹³⁹, H. Cai¹⁷⁰, V.M.M. Cairo²,
 O. Cakir^{4a}, N. Calace³⁵, P. Calafiura¹⁸, A. Calandri⁹⁹, G. Calderini¹³³, P. Calfayan⁶³, G. Callea⁵⁵,
 L.P. Caloba^{78b}, S. Calvente Lopez⁹⁶, D. Calvet³⁷, S. Calvet³⁷, T.P. Calvet¹⁵², M. Calvetti^{69a,69b},
 R. Camacho Toro¹³³, S. Camarda³⁵, D. Camarero Munoz⁹⁶, P. Camarri^{71a,71b}, D. Cameron¹³¹,
 R. Caminal Armadans¹⁰⁰, C. Camincher³⁵, S. Campana³⁵, M. Campanelli⁹², A. Camplani³⁹,
 A. Campoverde¹⁴⁸, V. Canale^{67a,67b}, M. Cano Bret^{58c}, J. Cantero¹²⁶, T. Cao¹⁵⁸, Y. Cao¹⁷⁰,
 M.D.M. Capeans Garrido³⁵, M. Capua^{40b,40a}, R.M. Carbone³⁸, R. Cardarelli^{71a}, F.C. Cardillo¹⁴⁶, I. Carli¹⁴⁰,
 T. Carli³⁵, G. Carlino^{67a}, B.T. Carlson¹³⁶, L. Carminati^{66a,66b}, R.M.D. Carney^{43a,43b}, S. Caron¹¹⁷,
 E. Carquin^{144b}, S. Carrá^{66a,66b}, J.W.S. Carter¹⁶⁴, D. Casadei^{32b}, M.P. Casado^{14,g}, A.F. Casha¹⁶⁴,
 D.W. Casper¹⁶⁸, R. Castelijns¹¹⁸, F.L. Castillo¹⁷¹, V. Castillo Gimenez¹⁷¹, N.F. Castro^{137a,137e},
 A. Catinaccio³⁵, J.R. Catmore¹³¹, A. Cattai³⁵, J. Caudron²⁴, V. Cavaliere^{26b}, E. Cavallaro¹⁴, D. Cavalli^{66a},
 M. Cavalli-Sforza¹⁴, V. Cavasinni^{69a,69b}, E. Celebi^{12b}, F. Ceradini^{72a,72b}, L. Cerda Alberich¹⁷¹,
 A.S. Cerqueira^{78a}, A. Cerri¹⁵³, L. Cerrito^{71a,71b}, F. Cerutti¹⁸, A. Cervelli^{23b,23a}, S.A. Cetin^{12b},
 A. Chafaq^{34a}, D. Chakraborty¹¹⁹, S.K. Chan⁵⁷, W.S. Chan¹¹⁸, W.Y. Chan⁸⁸, J.D. Chapman³¹,
 B. Chargeishvili^{156b}, D.G. Charlton²¹, C.C. Chau³³, C.A. Chavez Barajas¹⁵³, S. Che¹²³, A. Chegwidden¹⁰⁴,
 S. Chekanov⁶, S.V. Chekulaev^{165a}, G.A. Chelkov^{77,au}, M.A. Chelstowska³⁵, B. Chen⁷⁶, C. Chen^{58a},
 C.H. Chen⁷⁶, H. Chen^{26b}, J. Chen^{58a}, J. Chen³⁸, S. Chen¹³⁴, S.J. Chen^{15c}, X. Chen^{15b,at}, Y. Chen⁸⁰,
 Y-H. Chen⁴⁴, H.C. Cheng^{61a}, H.J. Cheng^{15d}, A. Cheplakov⁷⁷, E. Cheremushkina¹²¹,
 R. Cherkaoui El Moursli^{34e}, E. Cheu⁷, K. Cheung⁶², T.J.A. Chevaléras¹⁴², L. Chevalier¹⁴², V. Chiarella⁴⁹,
 G. Chiarelli^{69a}, G. Chiodini^{65a}, A.S. Chisholm^{35,21}, A. Chitan^{28b}, I. Chiu¹⁶⁰, Y.H. Chiu¹⁷³, M.V. Chizhov⁷⁷,
 K. Choi⁶³, A.R. Chomont¹²⁹, S. Chouridou¹⁵⁹, Y.S. Chow¹¹⁸, V. Christodoulou⁹², M.C. Chu^{61a},
 J. Chudoba¹³⁸, A.J. Chuinard¹⁰¹, J.J. Chwastowski⁸², L. Chytka¹²⁷, D. Cinca⁴⁵, V. Cindro⁸⁹, I.A. Cioară²⁴,
 A. Ciofalo¹⁸, F. Ciotto^{67a,67b}, Z.H. Citron¹⁷⁷, M. Citterio^{66a}, A. Clark⁵², M.R. Clark³⁸, P.J. Clark⁴⁸,
 C. Clement^{43a,43b}, Y. Coadou⁹⁹, M. Cobal^{64a,64c}, A. Coccaro^{53b}, J. Cochran⁷⁶, H. Cohen¹⁵⁸,
 A.E.C. Coimbra¹⁷⁷, L. Colasurdo¹¹⁷, B. Cole³⁸, A.P. Colijn¹¹⁸, J. Collot⁵⁶, P. Conde Muiño^{137a,h},
 E. Coniavitis⁵⁰, S.H. Connell^{32b}, I.A. Connelly⁹⁸, S. Constantinescu^{28b}, F. Conventi^{67a,ax},

A.M. Cooper-Sarkar¹³², F. Cormier¹⁷², K.J.R. Cormier¹⁶⁴, L.D. Corpe⁹², M. Corradi^{70a,70b}, E.E. Corrigan⁹⁴, F. Corriveau^{101,ac}, A. Cortes-Gonzalez³⁵, M.J. Costa¹⁷¹, F. Costanza⁵, D. Costanzo¹⁴⁶, G. Cottin³¹, G. Cowan⁹¹, J.W. Cowley³¹, B.E. Cox⁹⁸, J. Crane⁹⁸, K. Cranmer¹²², S.J. Crawley⁵⁵, R.A. Creager¹³⁴, G. Cree³³, S. Crépé-Renaudin⁵⁶, F. Crescioli¹³³, M. Cristinziani²⁴, V. Croft¹²², G. Crosetti^{40b,40a}, A. Cueto⁹⁶, T. Cuhadar Donszelmann¹⁴⁶, A.R. Cukierman¹⁵⁰, S. Czekierda⁸², P. Czodrowski³⁵, M.J. Da Cunha Sargedas De Sousa^{58b}, C. Da Via⁹⁸, W. Dabrowski^{81a}, T. Dado^{29a,x}, S. Dahbi^{34e}, T. Dai¹⁰³, F. Dallaire¹⁰⁷, C. Dallapiccola¹⁰⁰, M. Dam³⁹, G. D'amen^{23b,23a}, J. Damp⁹⁷, J.R. Dandoy¹³⁴, M.F. Daneri³⁰, N.P. Dang^{178,k}, N.D. Dann⁹⁸, M. Danninger¹⁷², V. Dao³⁵, G. Darbo^{53b}, S. Darmora⁸, O. Dartsis⁵, A. Dattagupta¹²⁸, T. Daubney⁴⁴, S. D'Auria^{66a,66b}, W. Davey²⁴, C. David⁴⁴, T. Davidek¹⁴⁰, D.R. Davis⁴⁷, E. Dawe¹⁰², I. Dawson¹⁴⁶, K. De⁸, R. De Asmundis^{67a}, A. De Benedetti¹²⁵, M. De Beurs¹¹⁸, S. De Castro^{23b,23a}, S. De Cecco^{70a,70b}, N. De Groot¹¹⁷, P. de Jong¹¹⁸, H. De la Torre¹⁰⁴, F. De Lorenzi⁷⁶, A. De Maria^{69a,69b}, D. De Pedis^{70a}, A. De Salvo^{70a}, U. De Sanctis^{71a,71b}, M. De Santis^{71a,71b}, A. De Santo¹⁵³, K. De Vasconcelos Corga⁹⁹, J.B. De Vivie De Regie¹²⁹, C. Debenedetti¹⁴³, D.V. Dedovich⁷⁷, N. Dehghanian³, M. Del Gaudio^{40b,40a}, J. Del Peso⁹⁶, Y. Delabat Diaz⁴⁴, D. Delgove¹²⁹, F. Deliot¹⁴², C.M. Delitzsch⁷, M. Della Pietra^{67a,67b}, D. Della Volpe⁵², A. Dell'Acqua³⁵, L. Dell'Asta²⁵, M. Delmastro⁵, C. Delporte¹²⁹, P.A. Delsart⁵⁶, D.A. DeMarco¹⁶⁴, S. Demers¹⁸⁰, M. Demichev⁷⁷, S.P. Denisov¹²¹, D. Denysiuk¹¹⁸, L. D'Eramo¹³³, D. Derendarz⁸², J.E. Derkaoui^{34d}, F. Derue¹³³, P. Dervan⁸⁸, K. Desch²⁴, C. Deterre⁴⁴, K. Dette¹⁶⁴, M.R. Devesa³⁰, P.O. Deviveiros³⁵, A. Dewhurst¹⁴¹, S. Dhaliwal²⁷, F.A. Di Bello⁵², A. Di Ciaccio^{71a,71b}, L. Di Ciaccio⁵, W.K. Di Clemente¹³⁴, C. Di Donato^{67a,67b}, A. Di Girolamo³⁵, G. Di Gregorio^{69a,69b}, B. Di Micco^{72a,72b}, R. Di Nardo¹⁰⁰, K.F. Di Petrillo⁵⁷, R. Di Sipio¹⁶⁴, D. Di Valentino³³, C. Diaconu⁹⁹, M. Diamond¹⁶⁴, F.A. Dias³⁹, T. Dias Do Vale^{137a}, M.A. Diaz^{144a}, J. Dickinson¹⁸, E.B. Diehl¹⁰³, J. Dietrich¹⁹, S. Díez Cornell⁴⁴, A. Dimitrievska¹⁸, J. Dingfelder²⁴, F. Dittus³⁵, F. Djama⁹⁹, T. Djobava^{156b}, J.I. Djuvsland¹⁷, M.A.B. Do Vale^{78c}, M. Dobre^{28b}, D. Dodsworth²⁷, C. Doglioni⁹⁴, J. Dolejsi¹⁴⁰, Z. Dolezal¹⁴⁰, M. Donadelli^{78d}, J. Donini³⁷, A. D'Onofrio⁹⁰, M. D'Onofrio⁸⁸, J. Dopke¹⁴¹, A. Doria^{67a}, M.T. Dova⁸⁶, A.T. Doyle⁵⁵, E. Drechsler¹⁴⁹, E. Dreyer¹⁴⁹, T. Dreyer⁵¹, Y. Du^{58b}, F. Dubinin¹⁰⁸, M. Dubovsky^{29a}, A. Dubreuil⁵², E. Duchovni¹⁷⁷, G. Duckeck¹¹², A. Ducourthial¹³³, O.A. Ducu^{107,w}, D. Duda¹¹³, A. Dudarev³⁵, A.C. Dudder⁹⁷, E.M. Duffield¹⁸, L. Duflot¹²⁹, M. Dührssen³⁵, C. Dülse¹⁷⁹, M. Dumancic¹⁷⁷, A.E. Dumitriu^{28b,e}, A.K. Duncan⁵⁵, M. Dunford^{59a}, A. Duperrin⁹⁹, H. Duran Yildiz^{4a}, M. Düren⁵⁴, A. Durglishvili^{156b}, D. Duschinger⁴⁶, B. Dutta⁴⁴, D. Duvnjak¹, G. Dyckes¹³⁴, M. Dyndal⁴⁴, S. Dysch⁹⁸, B.S. Dziedzic⁸², K.M. Ecker¹¹³, R.C. Edgar¹⁰³, T. Eifert³⁵, G. Eigen¹⁷, K. Einsweiler¹⁸, T. Ekelof¹⁶⁹, M. El Kacimi^{34c}, R. El Kosseifi⁹⁹, V. Ellajosyula⁹⁹, M. Ellert¹⁶⁹, F. Ellinghaus¹⁷⁹, A.A. Elliot⁹⁰, N. Ellis³⁵, J. Elmsheuser^{26b}, M. Elsing³⁵, D. Emeliyanov¹⁴¹, A. Emerman³⁸, Y. Enari¹⁶⁰, J.S. Ennis¹⁷⁵, M.B. Epland⁴⁷, J. Erdmann⁴⁵, A. Ereditato²⁰, S. Errede¹⁷⁰, M. Escalier¹²⁹, C. Escobar¹⁷¹, O. Estrada Pastor¹⁷¹, A.I. Etiennevire¹⁴², E. Etzion¹⁵⁸, H. Evans⁶³, A. Ezhilov¹³⁵, M. Ezzi^{34e}, F. Fabbri⁵⁵, L. Fabbri^{23b,23a}, V. Fabiani¹¹⁷, G. Facini⁹², R.M. Faisca Rodrigues Pereira^{137a}, R.M. Fakhrutdinov¹²¹, S. Falciano^{70a}, P.J. Falke⁵, S. Falke⁵, J. Faltova¹⁴⁰, Y. Fang^{15a}, M. Fanti^{66a,66b}, A. Farbin⁸, A. Farilla^{72a}, E.M. Farina^{68a,68b}, T. Farooque¹⁰⁴, S. Farrell¹⁸, S.M. Farrington¹⁷⁵, P. Farthouat³⁵, F. Fassi^{34e}, P. Fassnacht³⁵, D. Fassouliotis⁹, M. Fauci Giannelli⁴⁸, W.J. Fawcett³¹, L. Fayard¹²⁹, O.L. Fedin^{135,p}, W. Fedorko¹⁷², M. Feickert⁴¹, S. Feigl¹³¹, L. Feligioni⁹⁹, C. Feng^{58b}, E.J. Feng³⁵, M. Feng⁴⁷, M.J. Fenton⁵⁵, A.B. Fenyyuk¹²¹, J. Ferrando⁴⁴, A. Ferrari¹⁶⁹, P. Ferrari¹¹⁸, R. Ferrari^{68a}, D.E. Ferreira de Lima^{59b}, A. Ferrer¹⁷¹, D. Ferrere⁵², C. Ferretti¹⁰³, F. Fiedler⁹⁷, A. Filipčič⁸⁹, F. Filthaut¹¹⁷, K.D. Finelli²⁵, M.C.N. Fiolhais^{137a,137c,a}, L. Fiorini¹⁷¹, C. Fischer¹⁴, W.C. Fisher¹⁰⁴, N. Flaschel⁴⁴, I. Fleck¹⁴⁸, P. Fleischmann¹⁰³, R.R.M. Fletcher¹³⁴, T. Flick¹⁷⁹, B.M. Flierl¹¹², L.M. Flores¹³⁴, L.R. Flores Castillo^{61a}, F.M. Follega^{73a,73b}, N. Fomin¹⁷, G.T. Forcolin^{73a,73b}, A. Formica¹⁴², F.A. Förster¹⁴, A.C. Forti⁹⁸, A.G. Foster²¹, D. Fournier¹²⁹, H. Fox⁸⁷, S. Fracchia¹⁴⁶, P. Francavilla^{69a,69b}, M. Franchini^{23b,23a}, S. Franchino^{59a}, D. Francis³⁵, L. Franconi¹⁴³, M. Franklin⁵⁷, M. Frate¹⁶⁸, A.N. Fray⁹⁰, D. Freeborn⁹², B. Freund¹⁰⁷, W.S. Freund^{78b}, E.M. Freundlich⁴⁵, D.C. Frizzell¹²⁵, D. Froidevaux³⁵, J.A. Frost¹³², C. Fukunaga¹⁶¹, E. Fullana Torregrosa¹⁷¹, E. Fumagalli^{53b,53a}, T. Fusayasu¹¹⁴, J. Fuster¹⁷¹, O. Gabizon¹⁵⁷, A. Gabrielli^{23b,23a}, A. Gabrielli¹⁸, G.P. Gach^{81a}, S. Gadatsch⁵², P. Gadow¹¹³, G. Gagliardi^{53b,53a}, L.G. Gagnon¹⁰⁷, C. Galea^{28b}, B. Galhardo^{137a,137c}, E.J. Gallas¹³², B.J. Gallop¹⁴¹, P. Gallus¹³⁹, G. Galster³⁹, R. Gamboa Goni⁹⁰, K.K. Gan¹²³, S. Ganguly¹⁷⁷, J. Gao^{58a}, Y. Gao⁸⁸,

Y.S. Gao ^{150,m}, C. García ¹⁷¹, J.E. García Navarro ¹⁷¹, J.A. García Pascual ^{15a}, C. Garcia-Argos ⁵⁰, M. Garcia-Sciveres ¹⁸, R.W. Gardner ³⁶, N. Garelli ¹⁵⁰, S. Gargiulo ⁵⁰, V. Garonne ¹³¹, K. Gasnikova ⁴⁴, A. Gaudiello ^{53b,53a}, G. Gaudio ^{68a}, I.L. Gavrilenko ¹⁰⁸, A. Gavrilyuk ¹⁰⁹, C. Gay ¹⁷², G. Gaycken ²⁴, E.N. Gazis ¹⁰, C.N.P. Gee ¹⁴¹, J. Geisen ⁵¹, M. Geisen ⁹⁷, M.P. Geisler ^{59a}, C. Gemme ^{53b}, M.H. Genest ⁵⁶, C. Geng ¹⁰³, S. Gentile ^{70a,70b}, S. George ⁹¹, D. Gerbaudo ¹⁴, G. Gessner ⁴⁵, S. Ghasemi ¹⁴⁸, M. Ghasemi Bostanabad ¹⁷³, M. Ghneimat ²⁴, B. Giacobbe ^{23b}, S. Giagu ^{70a,70b}, N. Giangiacomi ^{23b,23a}, P. Giannetti ^{69a}, A. Giannini ^{67a,67b}, S.M. Gibson ⁹¹, M. Gignac ¹⁴³, D. Gillberg ³³, G. Gilles ¹⁷⁹, D.M. Gingrich ^{3,av}, M.P. Giordani ^{64a,64c}, F.M. Giorgi ^{23b}, P.F. Giraud ¹⁴², P. Giromini ⁵⁷, G. Giugliarelli ^{64a,64c}, D. Giugni ^{66a}, F. Giuli ¹³², M. Giulini ^{59b}, S. Gkaitatzis ¹⁵⁹, I. Gkialas ^{9,j}, E.L. Gkougkousis ¹⁴, P. Gkoutoumis ¹⁰, L.K. Gladilin ¹¹¹, C. Glasman ⁹⁶, J. Glatzer ¹⁴, P.C.F. Glaysheer ⁴⁴, A. Glazov ⁴⁴, M. Goblirsch-Kolb ²⁷, S. Goldfarb ¹⁰², T. Golling ⁵², D. Golubkov ¹²¹, A. Gomes ^{137a,137b}, R. Goncalves Gama ⁵¹, R. Gonçalo ^{137a}, G. Gonella ⁵⁰, L. Gonella ²¹, A. Gongadze ⁷⁷, F. Gonnella ²¹, J.L. Gonski ⁵⁷, S. González de la Hoz ¹⁷¹, S. Gonzalez-Sevilla ⁵², L. Goossens ³⁵, P.A. Gorbounov ¹⁰⁹, H.A. Gordon ^{26b}, B. Gorini ³⁵, E. Gorini ^{65a,65b}, A. Gorišek ⁸⁹, A.T. Goshaw ⁴⁷, C. Gössling ⁴⁵, M.I. Gostkin ⁷⁷, C.A. Gottardo ²⁴, C.R. Goudet ¹²⁹, D. Goujdami ^{34c}, A.G. Goussiou ¹⁴⁵, N. Govender ^{32b,c}, C. Goy ⁵, E. Gozani ¹⁵⁷, I. Grabowska-Bold ^{81a}, P.O.J. Gradin ¹⁶⁹, E.C. Graham ⁸⁸, J. Gramling ¹⁶⁸, E. Gramstad ¹³¹, S. Grancagnolo ¹⁹, V. Gratchev ¹³⁵, P.M. Gravila ^{28f}, F.G. Gravili ^{65a,65b}, C. Gray ⁵⁵, H.M. Gray ¹⁸, Z.D. Greenwood ^{93,ak}, C. Grefe ²⁴, K. Gregersen ⁹⁴, I.M. Gregor ⁴⁴, P. Grenier ¹⁵⁰, K. Grevtsov ⁴⁴, N.A. Grieser ¹²⁵, J. Griffiths ⁸, A.A. Grillo ¹⁴³, K. Grimm ^{150,b}, S. Grinstein ^{14,y}, Ph. Gris ³⁷, J.-F. Grivaz ¹²⁹, S. Groh ⁹⁷, E. Gross ¹⁷⁷, J. Grosse-Knetter ⁵¹, G.C. Grossi ⁹³, Z.J. Grout ⁹², C. Grud ¹⁰³, A. Grummer ¹¹⁶, L. Guan ¹⁰³, W. Guan ¹⁷⁸, J. Guenther ³⁵, A. Guerguichon ¹²⁹, F. Guescini ^{165a}, D. Guest ¹⁶⁸, R. Gugel ⁵⁰, B. Gui ¹²³, T. Guillemin ⁵, S. Guindon ³⁵, U. Gul ⁵⁵, J. Guo ^{58c}, W. Guo ¹⁰³, Y. Guo ^{58a,s}, Z. Guo ⁹⁹, R. Gupta ⁴⁴, S. Gurbuz ^{12c}, G. Gustavino ¹²⁵, P. Gutierrez ¹²⁵, C. Gutsche ⁹², C. Guyot ¹⁴², M.P. Guzik ^{81a}, C. Gwenlan ¹³², C.B. Gwilliam ⁸⁸, A. Haas ¹²², C. Haber ¹⁸, H.K. Hadavand ⁸, N. Haddad ^{34e}, A. Hadeef ^{58a}, S. Hageböck ²⁴, M. Hagihara ¹⁶⁶, M. Haleem ¹⁷⁴, J. Haley ¹²⁶, G. Halladjian ¹⁰⁴, G.D. Hallowell ⁹⁹, K. Hamacher ¹⁷⁹, P. Hamal ¹²⁷, K. Hamano ¹⁷³, A. Hamilton ^{32a}, G.N. Hamity ¹⁴⁶, K. Han ^{58a,qj}, L. Han ^{58a}, S. Han ^{15d}, K. Hanagaki ^{79,u}, M. Hance ¹⁴³, D.M. Handl ¹¹², B. Haney ¹³⁴, R. Hankache ¹³³, P. Hanke ^{59a}, E. Hansen ⁹⁴, J.B. Hansen ³⁹, J.D. Hansen ³⁹, M.C. Hansen ²⁴, P.H. Hansen ³⁹, E.C. Hanson ⁹⁸, K. Hara ¹⁶⁶, A.S. Hard ¹⁷⁸, T. Harenberg ¹⁷⁹, S. Harkusha ¹⁰⁵, P.F. Harrison ¹⁷⁵, N.M. Hartmann ¹¹², Y. Hasegawa ¹⁴⁷, A. Hasib ⁴⁸, S. Hassani ¹⁴², S. Haug ²⁰, R. Hauser ¹⁰⁴, L. Hauswald ⁴⁶, L.B. Havener ³⁸, M. Havranek ¹³⁹, C.M. Hawkes ²¹, R.J. Hawkings ³⁵, D. Hayden ¹⁰⁴, C. Hayes ¹⁵², C.P. Hays ¹³², J.M. Hays ⁹⁰, H.S. Hayward ⁸⁸, S.J. Haywood ¹⁴¹, F. He ^{58a}, M.P. Heath ⁴⁸, V. Hedberg ⁹⁴, L. Heelan ⁸, S. Heer ²⁴, K.K. Heidegger ⁵⁰, J. Heilman ³³, S. Heim ⁴⁴, T. Heim ¹⁸, B. Heinemann ^{44,aq}, J.J. Heinrich ¹¹², L. Heinrich ¹²², C. Heinz ⁵⁴, J. Hejbal ¹³⁸, L. Helary ³⁵, A. Held ¹⁷², S. Hellesund ¹³¹, C.M. Helling ¹⁴³, S. Hellman ^{43a,43b}, C. Helsens ³⁵, R.C.W. Henderson ⁸⁷, Y. Heng ¹⁷⁸, S. Henkelmann ¹⁷², A.M. Henriques Correia ³⁵, G.H. Herbert ¹⁹, H. Herde ²⁷, V. Herget ¹⁷⁴, Y. Hernández Jiménez ^{32c}, H. Herr ⁹⁷, M.G. Herrmann ¹¹², T. Herrmann ⁴⁶, G. Herten ⁵⁰, R. Hertenberger ¹¹², L. Hervas ³⁵, T.C. Herwig ¹³⁴, G.G. Hesketh ⁹², N.P. Hessey ^{165a}, A. Higashida ¹⁶⁰, S. Higashino ⁷⁹, E. Higón-Rodríguez ¹⁷¹, K. Hildebrand ³⁶, E. Hill ¹⁷³, J.C. Hill ³¹, K.K. Hill ^{26b}, K.H. Hiller ⁴⁴, S.J. Hillier ²¹, M. Hils ⁴⁶, I. Hinchliffe ¹⁸, F. Hinterkeuser ²⁴, M. Hirose ¹³⁰, D. Hirschbuehl ¹⁷⁹, B. Hiti ⁸⁹, O. Hladik ¹³⁸, D.R. Hlaluku ^{32c}, X. Hoad ⁴⁸, J. Hobbs ¹⁵², N. Hod ^{165a}, M.C. Hodgkinson ¹⁴⁶, A. Hoecker ³⁵, M.R. Hoferkamp ¹¹⁶, F. Hoenig ¹¹², D. Hohn ⁵⁰, D. Hohov ¹²⁹, T.R. Holmes ³⁶, M. Holzbock ¹¹², M. Homann ⁴⁵, L.B.A.H. Hommels ³¹, S. Honda ¹⁶⁶, T. Honda ⁷⁹, T.M. Hong ¹³⁶, A. Hönle ¹¹³, B.H. Hooberman ¹⁷⁰, W.H. Hopkins ¹²⁸, Y. Horii ¹¹⁵, P. Horn ⁴⁶, A.J. Horton ¹⁴⁹, L.A. Horyn ³⁶, J.-Y. Hostachy ⁵⁶, A. Hostiuc ¹⁴⁵, S. Hou ¹⁵⁵, A. Hoummada ^{34a}, J. Howarth ⁹⁸, J. Hoya ⁸⁶, M. Hrabovsky ¹²⁷, J. Hrdinka ³⁵, I. Hristova ¹⁹, J. Hrivnac ¹²⁹, A. Hrynevich ¹⁰⁶, T. Hryn'ova ⁵, P.J. Hsu ⁶², S.-C. Hsu ¹⁴⁵, Q. Hu ^{26b}, S. Hu ^{58c}, Y. Huang ^{15a}, Z. Hubacek ¹³⁹, F. Hubaut ⁹⁹, M. Huebner ²⁴, F. Huegging ²⁴, T.B. Huffman ¹³², M. Huhtinen ³⁵, R.F.H. Hunter ³³, P. Huo ¹⁵², A.M. Hupe ³³, N. Huseynov ^{77,ae}, J. Huston ¹⁰⁴, J. Huth ⁵⁷, R. Hyneman ¹⁰³, G. Iacobucci ⁵², G. Iakovidis ^{26b}, I. Ibragimov ¹⁴⁸, L. Iconomidou-Fayard ¹²⁹, Z. Idrissi ^{34e}, P. Iengo ³⁵, R. Ignazzi ³⁹, O. Igonkina ^{118,aa}, R. Iguchi ¹⁶⁰, T. Iizawa ⁵², Y. Ikegami ⁷⁹, M. Ikeno ⁷⁹, D. Iliadis ¹⁵⁹, N. Ilic ¹¹⁷, F. Iltzsche ⁴⁶, G. Introzzi ^{68a,68b}, M. Iodice ^{72a}, K. Iordanidou ³⁸, V. Ippolito ^{70a,70b}, M.F. Isacson ¹⁶⁹, N. Ishijima ¹³⁰, M. Ishino ¹⁶⁰, M. Ishitsuka ¹⁶², W. Islam ¹²⁶, C. Issever ¹³², S. Istin ¹⁵⁷, F. Ito ¹⁶⁶, J.M. Iturbe Ponce ^{61a},

R. Iuppa^{73a,73b}, A. Ivina¹⁷⁷, H. Iwasaki⁷⁹, J.M. Izen⁴², V. Izzo^{67a}, P. Jacka¹³⁸, P. Jackson¹, R.M. Jacobs²⁴, V. Jain², G. Jäkel¹⁷⁹, K.B. Jakobi⁹⁷, K. Jakobs⁵⁰, S. Jakobsen⁷⁴, T. Jakoubek¹³⁸, D.O. Jamin¹²⁶, R. Jansky⁵², J. Janssen²⁴, M. Janus⁵¹, P.A. Janus^{81a}, G. Jarlskog⁹⁴, N. Javadov^{77,ae}, T. Javůrek³⁵, M. Javurkova⁵⁰, F. Jeanneau¹⁴², L. Jeanty¹⁸, J. Jejelava^{156a,af}, A. Jelinskas¹⁷⁵, P. Jenni^{50,d}, J. Jeong⁴⁴, N. Jeong⁴⁴, S. Jézéquel⁵, H. Ji¹⁷⁸, J. Jia¹⁵², H. Jiang⁷⁶, Y. Jiang^{58a}, Z. Jiang^{150,q}, S. Jiggins⁵⁰, F.A. Jimenez Morales³⁷, J. Jimenez Pena¹⁷¹, S. Jin^{15c}, A. Jinaru^{28b}, O. Jinnouchi¹⁶², H. Jivan^{32c}, P. Johansson¹⁴⁶, K.A. Johns⁷, C.A. Johnson⁶³, K. Jon-And^{43a,43b}, R.W.L. Jones⁸⁷, S.D. Jones¹⁵³, S. Jones⁷, T.J. Jones⁸⁸, J. Jongmanns^{59a}, P.M. Jorge^{137a,137b}, J. Jovicevic^{165a}, X. Ju¹⁸, J.J. Junggeburth¹¹³, A. Juste Rozas^{14,y}, A. Kaczmarska⁸², M. Kado¹²⁹, H. Kagan¹²³, M. Kagan¹⁵⁰, T. Kaji¹⁷⁶, E. Kajomovitz¹⁵⁷, C.W. Kalderon⁹⁴, A. Kaluza⁹⁷, S. Kama⁴¹, A. Kamenshchikov¹²¹, L. Kanjir⁸⁹, Y. Kano¹⁶⁰, V.A. Kantserov¹¹⁰, J. Kanzaki⁷⁹, L.S. Kaplan¹⁷⁸, D. Kar^{32c}, M.J. Kareem^{165b}, E. Karentzos¹⁰, S.N. Karpov⁷⁷, Z.M. Karpova⁷⁷, V. Kartvelishvili⁸⁷, A.N. Karyukhin¹²¹, L. Kashif¹⁷⁸, R.D. Kass¹²³, A. Kastanas^{43a,43b}, Y. Kataoka¹⁶⁰, C. Kato^{58d,58c}, J. Katzy⁴⁴, K. Kawade⁸⁰, K. Kawagoe⁸⁵, T. Kawaguchi¹¹⁵, T. Kawamoto¹⁶⁰, G. Kawamura⁵¹, E.F. Kay⁸⁸, V.F. Kazanin^{120b,120a}, R. Keeler¹⁷³, R. Kehoe⁴¹, J.S. Keller³³, E. Kellermann⁹⁴, J.J. Kempster²¹, J. Kendrick²¹, O. Kepka¹³⁸, S. Kersten¹⁷⁹, B.P. Kerševan⁸⁹, S. Ketabchi Haghighat¹⁶⁴, R.A. Keyes¹⁰¹, M. Khader¹⁷⁰, F. Khalil-Zada¹³, A. Khanov¹²⁶, A.G. Kharlamov^{120b,120a}, T. Kharlamova^{120b,120a}, E.E. Khoda¹⁷², A. Khodinov¹⁶³, T.J. Khoo⁵², E. Khramov⁷⁷, J. Khubua^{156b}, S. Kido⁸⁰, M. Kiehn⁵², C.R. Kilby⁹¹, Y.K. Kim³⁶, N. Kimura^{64a,64c}, O.M. Kind¹⁹, B.T. King⁸⁸, D. Kirchmeier⁴⁶, J. Kirk¹⁴¹, A.E. Kiryunin¹¹³, T. Kishimoto¹⁶⁰, V. Kitali⁴⁴, O. Kivernyk⁵, E. Kladiva^{29b,*}, T. Klapdor-Kleingrothaus⁵⁰, M.H. Klein¹⁰³, M. Klein⁸⁸, U. Klein⁸⁸, K. Kleinknecht⁹⁷, P. Klimek¹¹⁹, A. Klimentov^{26b}, T. Klingl²⁴, T. Klioutchnikova³⁵, F.F. Klitzner¹¹², P. Kluit¹¹⁸, S. Kluth¹¹³, E. Kneringer⁷⁴, E.B.F.G. Knoops⁹⁹, A. Knue⁵⁰, A. Kobayashi¹⁶⁰, D. Kobayashi⁸⁵, T. Kobayashi¹⁶⁰, M. Kobel⁴⁶, M. Kocian¹⁵⁰, P. Kodys¹⁴⁰, P.T. Koenig²⁴, T. Koffas³³, E. Koffeman¹¹⁸, N.M. Köhler¹¹³, T. Koi¹⁵⁰, M. Kolb^{59b}, I. Koletsou⁵, T. Kondo⁷⁹, N. Kondrashova^{58c}, K. Köneke⁵⁰, A.C. König¹¹⁷, T. Kono⁷⁹, R. Konoplich^{122,am}, V. Konstantinides⁹², N. Konstantinidis⁹², B. Konya⁹⁴, R. Kopeliansky⁶³, S. Koperny^{81a}, K. Korcyl⁸², K. Kordas¹⁵⁹, G. Koren¹⁵⁸, A. Korn⁹², I. Korolkov¹⁴, E.V. Korolkova¹⁴⁶, N. Korotkova¹¹¹, O. Kortner¹¹³, S. Kortner¹¹³, T. Kosek¹⁴⁰, V.V. Kostyukhin²⁴, A. Kotwal⁴⁷, A. Koulouris¹⁰, A. Kourkoulis-Charalampidi^{68a,68b}, C. Kourkoulis⁹, E. Kourlitis¹⁴⁶, V. Kouskoura^{26b}, A.B. Kowalewska⁸², R. Kowalewski¹⁷³, C. Kozakai¹⁶⁰, W. Kozanecki¹⁴², A.S. Kozhin¹²¹, V.A. Kramarenko¹¹¹, G. Kramberger⁸⁹, D. Krasnopevtsev^{58a}, M.W. Krasny¹³³, A. Krasznahorkay³⁵, D. Krauss¹¹³, J.A. Kremer^{81a}, J. Kretzschmar⁸⁸, P. Krieger¹⁶⁴, K. Krizka¹⁸, K. Kroeninger⁴⁵, H. Kroha¹¹³, J. Kroll¹³⁸, J. Kroll¹³⁴, J. Krstic¹⁶, U. Kruchonak⁷⁷, H. Krüger²⁴, N. Krumnack⁷⁶, M.C. Kruse⁴⁷, T. Kubota¹⁰², S. Kuday^{4b}, J.T. Kuechler¹⁷⁹, S. Kuehn³⁵, A. Kugel^{59a}, T. Kuhl⁴⁴, V. Kukhtin⁷⁷, R. Kukla⁹⁹, Y. Kulchitsky^{105,ai}, S. Kuleshov^{144b}, Y.P. Kulinich¹⁷⁰, M. Kuna⁵⁶, T. Kunigo⁸³, A. Kupco¹³⁸, T. Kupfer⁴⁵, O. Kuprash¹⁵⁸, H. Kurashige⁸⁰, L.L. Kurchaninov^{165a}, Y.A. Kurochkin¹⁰⁵, A. Kurova¹¹⁰, M.G. Kurth^{15d}, E.S. Kuwertz³⁵, M. Kuze¹⁶², J. Kvita¹²⁷, T. Kwan¹⁰¹, A. La Rosa¹¹³, J.L. La Rosa Navarro^{78d}, L. La Rotonda^{40b,40a}, F. La Ruffa^{40b,40a}, C. Lacasta¹⁷¹, F. Lacava^{70a,70b}, J. Lacey⁴⁴, D.P.J. Lack⁹⁸, H. Lacker¹⁹, D. Lacour¹³³, E. Ladygin⁷⁷, R. Lafaye⁵, B. Laforge¹³³, T. Lagouri^{32c}, S. Lai⁵¹, S. Lammers⁶³, W. Lampl⁷, E. Lançon^{26b}, U. Landgraf⁵⁰, M.P.J. Landon⁹⁰, M.C. Lanfermann⁵², V.S. Lang⁴⁴, J.C. Lange⁵¹, R.J. Langenberg³⁵, A.J. Lankford¹⁶⁸, F. Lanni^{26b}, K. Lantzsch²⁴, A. Lanza^{68a}, A. Lapertosa^{53b,53a}, S. Laplace¹³³, J.F. Laporte¹⁴², T. Lari^{66a}, F. Lasagni Manghi^{23b,23a}, M. Lassnig³⁵, T.S. Lau^{61a}, A. Laudrain¹²⁹, M. Lavorgna^{67a,67b}, M. Lazzaroni^{66a,66b}, B. Le¹⁰², O. Le Dortz¹³³, E. Le Guirriec⁹⁹, E.P. Le Quilleuc¹⁴², M. LeBlanc⁷, T. LeCompte⁶, F. Ledroit-Guillon⁵⁶, C.A. Lee^{26b}, G.R. Lee^{144a}, L. Lee⁵⁷, S.C. Lee¹⁵⁵, B. Lefebvre¹⁰¹, M. Lefebvre¹⁷³, F. Legger¹¹², C. Leggett¹⁸, K. Lehmann¹⁴⁹, N. Lehmann¹⁷⁹, G. Lehmann Miotto³⁵, W.A. Leight⁴⁴, A. Leisos^{159,v}, M.A.L. Leite^{78d}, R. Leitner¹⁴⁰, D. Lellouch¹⁷⁷, K.J.C. Leney⁹², T. Lenz²⁴, B. Lenzi³⁵, R. Leone⁷, S. Leone^{69a}, C. Leonidopoulos⁴⁸, G. Lerner¹⁵³, C. Leroy¹⁰⁷, R. Les¹⁶⁴, A.A.J. Lesage¹⁴², C.G. Lester³¹, M. Levchenko¹³⁵, J. Levêque⁵, D. Levin¹⁰³, L.J. Levinson¹⁷⁷, D. Lewis⁹⁰, B. Li^{15b}, B. Li¹⁰³, C.-Q. Li^{58a,al}, H. Li^{58a}, H. Li^{58b}, K. Li¹⁵⁰, L. Li^{58c}, M. Li^{15a}, Q. Li^{15d}, Q.Y. Li^{58a}, S. Li^{58d,58c}, X. Li^{58c}, Y. Li¹⁴⁸, Z. Liang^{15a}, B. Liberti^{71a}, A. Liblong¹⁶⁴, K. Lie^{61c}, S. Liem¹¹⁸, A. Limosani¹⁵⁴, C.Y. Lin³¹, K. Lin¹⁰⁴, T.H. Lin⁹⁷, R.A. Linck⁶³, J.H. Lindon²¹, B.E. Lindquist¹⁵², A.L. Lioni⁵², E. Lipeles¹³⁴, A. Lipniacka¹⁷, M. Lisovsky^{59b}, T.M. Liss^{170,as}, A. Lister¹⁷², A.M. Litke¹⁴³, J.D. Little⁸, B. Liu⁷⁶, B.L. Liu⁶, H.B. Liu^{26b}, H. Liu¹⁰³, J.B. Liu^{58a}, J.K.K. Liu¹³², K. Liu¹³³, M. Liu^{58a},

P. Liu ¹⁸, Y. Liu ^{15a}, Y.L. Liu ^{58a}, Y.W. Liu ^{58a}, M. Livan ^{68a,68b}, A. Lleres ⁵⁶, J. Llorente Merino ^{15a}, S.L. Lloyd ⁹⁰, C.Y. Lo ^{61b}, F. Lo Sterzo ⁴¹, E.M. Lobodzinska ⁴⁴, P. Loch ⁷, T. Lohse ¹⁹, K. Lohwasser ¹⁴⁶, M. Lokajicek ¹³⁸, J.D. Long ¹⁷⁰, R.E. Long ⁸⁷, L. Longo ^{65a,65b}, K.A. Looper ¹²³, J.A. Lopez ^{144b}, I. Lopez Paz ⁹⁸, A. Lopez Solis ¹⁴⁶, J. Lorenz ¹¹², N. Lorenzo Martinez ⁵, M. Losada ²², P.J. Lösel ¹¹², A. Lösle ⁵⁰, X. Lou ⁴⁴, X. Lou ^{15a}, A. Lounis ¹²⁹, J. Love ⁶, P.A. Love ⁸⁷, J.J. Lozano Bahilo ¹⁷¹, H. Lu ^{61a}, M. Lu ^{58a}, Y.J. Lu ⁶², H.J. Lubatti ¹⁴⁵, C. Luci ^{70a,70b}, A. Lucotte ⁵⁶, C. Luedtke ⁵⁰, F. Luehring ⁶³, I. Luise ¹³³, L. Luminari ^{70a}, B. Lund-Jensen ¹⁵¹, M.S. Lutz ¹⁰⁰, P.M. Luzi ¹³³, D. Lynn ^{26b}, R. Lysak ¹³⁸, E. Lytken ⁹⁴, F. Lyu ^{15a}, V. Lyubushkin ⁷⁷, T. Lyubushkina ⁷⁷, H. Ma ^{26b}, L.L. Ma ^{58b}, Y. Ma ^{58b}, G. Maccarrone ⁴⁹, A. Macchiolo ¹¹³, C.M. Macdonald ¹⁴⁶, J. Machado Miguens ^{134,137b}, D. Madaffari ¹⁷¹, R. Madar ³⁷, W.F. Mader ⁴⁶, N. Madysa ⁴⁶, J. Maeda ⁸⁰, K. Maekawa ¹⁶⁰, S. Maeland ¹⁷, T. Maeno ^{26b}, M. Maerker ⁴⁶, A.S. Maevskiy ¹¹¹, V. Magerl ⁵⁰, D.J. Mahon ³⁸, C. Maidantchik ^{78b}, T. Maier ¹¹², A. Maio ^{137a,137b,137d}, O. Majersky ^{29a}, S. Majewski ¹²⁸, Y. Makida ⁷⁹, N. Makovec ¹²⁹, B. Malaescu ¹³³, Pa. Malecki ⁸², V.P. Maleev ¹³⁵, F. Malek ⁵⁶, U. Mallik ⁷⁵, D. Malon ⁶, C. Malone ³¹, S. Maltezos ¹⁰, S. Malyukov ³⁵, J. Mamuzic ¹⁷¹, G. Mancini ⁴⁹, I. Mandić ⁸⁹, J. Maneira ^{137a}, L. Manhaes de Andrade Filho ^{78a}, J. Manjarres Ramos ⁴⁶, K.H. Mankinen ⁹⁴, A. Mann ¹¹², A. Manousos ⁷⁴, B. Mansoulie ¹⁴², S. Manzoni ^{66a,66b}, A. Marantis ¹⁵⁹, G. Marceca ³⁰, L. March ⁵², L. Marchese ¹³², G. Marchiori ¹³³, M. Marcisovsky ¹³⁸, C. Marcon ⁹⁴, C.A. Marin Tobon ³⁵, M. Marjanovic ³⁷, F. Marroquim ^{78b}, Z. Marshall ¹⁸, M.U.F. Martensson ¹⁶⁹, S. Marti-Garcia ¹⁷¹, C.B. Martin ¹²³, T.A. Martin ¹⁷⁵, V.J. Martin ⁴⁸, B. Martin dit Latour ¹⁷, M. Martinez ^{14,y}, V.I. Martinez Outschoorn ¹⁰⁰, S. Martin-Haugh ¹⁴¹, V.S. Martoiu ^{28b}, A.C. Martyniuk ⁹², A. Marzin ³⁵, L. Masetti ⁹⁷, T. Mashimo ¹⁶⁰, R. Mashinistov ¹⁰⁸, J. Masik ⁹⁸, A.L. Maslennikov ^{120b,120a}, L.H. Mason ¹⁰², L. Massa ^{71a,71b}, P. Massarotti ^{67a,67b}, P. Mastrandrea ¹⁵², A. Mastroberardino ^{40b,40a}, T. Masubuchi ¹⁶⁰, P. Mättig ²⁴, J. Maurer ^{28b}, B. Maček ⁸⁹, S.J. Maxfield ⁸⁸, D.A. Maximov ^{120b,120a}, R. Mazini ¹⁵⁵, I. Maznas ¹⁵⁹, S.M. Mazza ¹⁴³, S.P. Mc Kee ¹⁰³, A. McCarn Deiana ⁴¹, T.G. McCarthy ¹¹³, L.I. McClymont ⁹², W.P. McCormack ¹⁸, E.F. McDonald ¹⁰², J.A. Mcfayden ³⁵, G. Mchedlidze ⁵¹, M.A. McKay ⁴¹, K.D. McLean ¹⁷³, S.J. McMahon ¹⁴¹, P.C. McNamara ¹⁰², C.J. McNicol ¹⁷⁵, R.A. McPherson ^{173,ac}, J.E. Mdhluli ^{32c}, Z.A. Meadows ¹⁰⁰, S. Meehan ¹⁴⁵, T.M. Megy ⁵⁰, S. Mehlhase ¹¹², A. Mehta ⁸⁸, T. Meideck ⁵⁶, B. Meirose ⁴², D. Melini ^{171,aw}, B.R. Mellado Garcia ^{32c}, J.D. Mellenthin ⁵¹, M. Melo ^{29a}, F. Meloni ⁴⁴, A. Melzer ²⁴, S.B. Menary ⁹⁸, E.D. Mendes Gouveia ^{137a}, L. Meng ⁸⁸, X.T. Meng ¹⁰³, S. Menke ¹¹³, E. Meoni ^{40b,40a}, S. Mergelmeyer ¹⁹, S.A.M. Merkt ¹³⁶, C. Merlassino ²⁰, P. Mermod ⁵², L. Merola ^{67a,67b}, C. Meroni ^{66a}, A. Messina ^{70a,70b}, J. Metcalfe ⁶, A.S. Mete ¹⁶⁸, C. Meyer ⁶³, J. Meyer ¹⁵⁷, J.-P. Meyer ¹⁴², H. Meyer Zu Theenhausen ^{59a}, F. Miano ¹⁵³, R.P. Middleton ¹⁴¹, L. Mijović ⁴⁸, G. Mikenberg ¹⁷⁷, M. Mikestikova ¹³⁸, M. Mikuž ⁸⁹, M. Milesi ¹⁰², A. Milic ¹⁶⁴, D.A. Millar ⁹⁰, D.W. Miller ³⁶, A. Milov ¹⁷⁷, D.A. Milstead ^{43a,43b}, R.A. Mina ^{150,q}, A.A. Minaenko ¹²¹, M. Miñano Moya ¹⁷¹, I.A. Minashvili ^{156b}, A.I. Mincer ¹²², B. Mindur ^{81a}, M. Mineev ⁷⁷, Y. Minegishi ¹⁶⁰, Y. Ming ¹⁷⁸, L.M. Mir ¹⁴, A. Mirto ^{65a,65b}, K.P. Mistry ¹³⁴, T. Mitani ¹⁷⁶, J. Mitrevski ¹¹², V.A. Mitsou ¹⁷¹, M. Mittal ^{58c}, A. Miucci ²⁰, P.S. Miyagawa ¹⁴⁶, A. Mizukami ⁷⁹, J.U. Mjörnmark ⁹⁴, T. Mkrtchyan ¹⁸¹, M. Mlynarikova ¹⁴⁰, T. Moa ^{43a,43b}, K. Mochizuki ¹⁰⁷, P. Mogg ⁵⁰, S. Mohapatra ³⁸, S. Molander ^{43a,43b}, R. Moles-Valls ²⁴, M.C. Mondragon ¹⁰⁴, K. Mönig ⁴⁴, J. Monk ³⁹, E. Monnier ⁹⁹, A. Montalbano ¹⁴⁹, J. Montejo Berlingen ³⁵, F. Monticelli ⁸⁶, S. Monzani ^{66a}, N. Morange ¹²⁹, D. Moreno ²², M. Moreno Llácer ³⁵, P. Morettini ^{53b}, M. Morgenstern ¹¹⁸, S. Morgenstern ⁴⁶, D. Mori ¹⁴⁹, M. Morii ⁵⁷, M. Morinaga ¹⁷⁶, V. Morisbak ¹³¹, A.K. Morley ³⁵, G. Mornacchi ³⁵, A.P. Morris ⁹², J.D. Morris ⁹⁰, L. Morvaj ¹⁵², P. Moschovakos ¹⁰, M. Mosidze ^{156b}, H.J. Moss ¹⁴⁶, J. Moss ^{150,n}, K. Motohashi ¹⁶², R. Mount ¹⁵⁰, E. Mountricha ³⁵, E.J.W. Moyse ¹⁰⁰, S. Muanza ⁹⁹, F. Mueller ¹¹³, J. Mueller ¹³⁶, R.S.P. Mueller ¹¹², D. Muenstermann ⁸⁷, G.A. Mullier ⁹⁴, F.J. Munoz Sanchez ⁹⁸, P. Murin ^{29b}, W.J. Murray ^{175,141}, A. Murrone ^{66a,66b}, M. Muškinja ⁸⁹, C. Mwewa ^{32a}, A.G. Myagkov ^{121,an}, J. Myers ¹²⁸, M. Myska ¹³⁹, B.P. Nachman ¹⁸, O. Nackenhorst ⁴⁵, K. Nagai ¹³², K. Nagano ⁷⁹, Y. Nagasaka ⁶⁰, M. Nagel ⁵⁰, E. Nagy ⁹⁹, A.M. Nairz ³⁵, Y. Nakahama ¹¹⁵, K. Nakamura ⁷⁹, T. Nakamura ¹⁶⁰, I. Nakano ¹²⁴, H. Nanjo ¹³⁰, F. Napolitano ^{59a}, R.F. Naranjo Garcia ⁴⁴, R. Narayan ¹¹, D.I. Narrias Villar ^{59a}, I. Naryshkin ¹³⁵, T. Naumann ⁴⁴, G. Navarro ²², R. Nayyar ⁷, H.A. Neal ^{103,*}, P.Y. Nechaeva ¹⁰⁸, T.J. Neep ¹⁴², A. Negri ^{68a,68b}, M. Negrini ^{23b}, S. Nektarijevic ¹¹⁷, C. Nellist ⁵¹, M.E. Nelson ¹³², S. Nemecek ¹³⁸, P. Nemethy ¹²², M. Nessi ^{35,f}, M.S. Neubauer ¹⁷⁰, M. Neumann ¹⁷⁹, P.R. Newman ²¹, T.Y. Ng ^{61c}, Y.S. Ng ¹⁹, Y.W.Y. Ng ¹⁶⁸, H.D.N. Nguyen ⁹⁹, T. Nguyen Manh ¹⁰⁷, E. Nibigira ³⁷, R.B. Nickerson ¹³², R. Nicolaidou ¹⁴², D.S. Nielsen ³⁹, J. Nielsen ¹⁴³, N. Nikiforou ¹¹, V. Nikolaenko ^{121,an},

I. Nikolic-Audit¹³³, K. Nikolopoulos²¹, P. Nilsson^{26b}, H.R. Nindhito⁵², Y. Ninomiya⁷⁹, A. Nisati^{70a}, N. Nishu^{58c}, R. Nisius¹¹³, I. Nitsche⁴⁵, T. Nitta¹⁷⁶, T. Nobe¹⁶⁰, Y. Noguchi⁸³, M. Nomachi¹³⁰, I. Nomidis¹³³, M.A. Nomura^{26b}, T. Nooney⁹⁰, M. Nordberg³⁵, N. Norjoharuddeen¹³², T. Novak⁸⁹, O. Novgorodova⁴⁶, R. Novotny¹³⁹, L. Nozka¹²⁷, K. Ntekas¹⁶⁸, E. Nurse⁹², F. Nuti¹⁰², F.G. Oakham^{33,av}, H. Oberlack¹¹³, J. Ocariz¹³³, A. Ochi⁸⁰, I. Ochoa³⁸, J.P. Ochoa-Ricoux^{144a}, K. O'Connor²⁷, S. Oda⁸⁵, S. Odaka⁷⁹, S. Oerdek⁵¹, A. Oh⁹⁸, S.H. Oh⁴⁷, C.C. Ohm¹⁵¹, H. Oide^{53b,53a}, M.L. Ojeda¹⁶⁴, H. Okawa¹⁶⁶, Y. Okazaki⁸³, Y. Okumura¹⁶⁰, T. Okuyama⁷⁹, A. Olariu^{28b}, L.F. Oleiro Seabra^{137a}, S.A. Olivares Pino^{144a}, D. Oliveira Damazio^{26b}, J.L. Oliver¹, M.J.R. Olsson³⁶, A. Olszewski⁸², J. Olszowska⁸², D.C. O'Neil¹⁴⁹, A. Onofre^{137a,137e}, K. Onogi¹¹⁵, P.U.E. Onyisi¹¹, H. Oppen¹³¹, M.J. Oreglia³⁶, G.E. Orellana⁸⁶, Y. Oren¹⁵⁸, D. Orestano^{72a,72b}, N. Orlando^{61b}, A.A. O'Rourke⁴⁴, R.S. Orr¹⁶⁴, B. Osculati^{53b,53a,*}, V. O'Shea⁵⁵, R. Ospanov^{58a}, G. Otero y Garzon³⁰, H. Otono⁸⁵, M. Ouchrif^{34d}, J. Ouellette^{26a}, F. Ould-Saada¹³¹, A. Ouraou¹⁴², Q. Ouyang^{15a}, M. Owen⁵⁵, R.E. Owen²¹, V.E. Ozcan^{12c}, N. Ozturk⁸, J. Pacalt¹²⁷, H.A. Pacey³¹, K. Pachal¹⁴⁹, A. Pacheco Pages¹⁴, L. Pacheco Rodriguez¹⁴², C. Padilla Aranda¹⁴, S. Pagan Griso¹⁸, M. Paganini¹⁸⁰, G. Palacino⁶³, S. Palazzo⁴⁸, S. Palestini³⁵, M. Palka^{81b}, D. Pallin³⁷, I. Panagoulas¹⁰, C.E. Pandini³⁵, J.G. Panduro Vazquez⁹¹, P. Pani³⁵, G. Panizzo^{64a,64c}, L. Paolozzi⁵², K. Papageorgiou^{9,j}, A. Paramonov⁶, D. Paredes Hernandez^{61b}, S.R. Paredes Saenz¹³², B. Parida¹⁶³, T.H. Park³³, A.J. Parker⁸⁷, K.A. Parker⁴⁴, M.A. Parker³¹, F. Parodi^{53b,53a}, J.A. Parsons³⁸, U. Parzefall⁵⁰, V.R. Pascuzzi¹⁶⁴, J.M.P. Pasner¹⁴³, E. Pasqualucci^{70a}, S. Passaggio^{53b}, F. Pastore⁹¹, P. Pasuwan^{43a,43b}, S. Pataria⁹⁷, J.R. Pater⁹⁸, A. Pathak^{178,k}, T. Pauly³⁵, B. Pearson¹¹³, M. Pedersen¹³¹, L. Pedraza Diaz¹¹⁷, R. Pedro^{137a,137b}, S.V. Peleganchuk^{120b,120a}, O. Penc¹³⁸, C. Peng^{15d}, H. Peng^{58a}, B.S. Peralva^{78a}, M.M. Perego¹²⁹, A.P. Pereira Peixoto^{137a}, D.V. Perepelitsa^{26b}, F. Peri¹⁹, L. Perini^{66a,66b}, H. Pernegger³⁵, S. Perrella^{67a,67b}, V.D. Peshekhonov^{77,*}, K. Peters⁴⁴, R.F.Y. Peters⁹⁸, B.A. Petersen³⁵, T.C. Petersen³⁹, E. Petit⁵⁶, A. Petridis¹, C. Petridou¹⁵⁹, P. Petroff¹²⁹, M. Petrov¹³², F. Petrucci^{72a,72b}, M. Pettee¹⁸⁰, N.E. Pettersson¹⁰⁰, A. Peyaud¹⁴², R. Pezoa^{144b}, T. Pham¹⁰², F.H. Phillips¹⁰⁴, P.W. Phillips¹⁴¹, M.W. Phipps¹⁷⁰, G. Piacquadio¹⁵², E. Pianori¹⁸, A. Picazio¹⁰⁰, R.H. Pickles⁹⁸, R. Piegaia³⁰, J.E. Pilcher³⁶, A.D. Pilkington⁹⁸, M. Pinamonti^{71a,71b}, J.L. Pinfold³, M. Pitt¹⁷⁷, L. Pizzimento^{71a,71b}, M.-A. Pleier^{26b}, V. Pleskot¹⁴⁰, E. Plotnikova⁷⁷, D. Pluth⁷⁶, P. Podberezko^{120b,120a}, R. Poettgen⁹⁴, R. Poggi⁵², L. Poggioli¹²⁹, I. Pogrebnyak¹⁰⁴, D. Pohl²⁴, I. Pokharel⁵¹, G. Polesello^{68a}, A. Poley¹⁸, A. Policicchio^{70a,70b}, R. Polifka³⁵, A. Polini^{23b}, C.S. Pollard⁴⁴, V. Polychronakos^{26b}, D. Ponomarenko¹¹⁰, L. Pontecorvo³⁵, G.A. Popeneciu^{28d}, D.M. Portillo Quintero¹³³, S. Pospisil¹³⁹, K. Potamianos⁴⁴, I.N. Potrap⁷⁷, C.J. Potter³¹, H. Potti¹¹, T. Poulsen⁹⁴, J. Poveda³⁵, T.D. Powell¹⁴⁶, M.E. Pozo Astigarraga³⁵, P. Pralavorio⁹⁹, S. Prell⁷⁶, D. Price⁹⁸, M. Primavera^{65a}, S. Prince¹⁰¹, M.L. Proffitt¹⁴⁵, N. Proklova¹¹⁰, K. Prokofiev^{61c}, F. Prokoshin^{144b}, S. Protopopescu^{26b}, J. Proudfoot⁶, M. Przybycien^{81a}, A. Puri¹⁷⁰, P. Puzo¹²⁹, J. Qian¹⁰³, Y. Qin⁹⁸, A. Quadt⁵¹, M. Queitsch-Maitland⁴⁴, A. Qureshi¹, P. Rados¹⁰², F. Ragusa^{66a,66b}, G. Rahal⁹⁵, J.A. Raine⁵², S. Rajagopalan^{26b}, A. Ramirez Morales⁹⁰, K. Ran^{15a}, T. Rashid¹²⁹, S. Raspopov⁵, M.G. Ratti^{66a,66b}, D.M. Rauch⁴⁴, F. Rauscher¹¹², S. Rave⁹⁷, B. Ravina¹⁴⁶, I. Ravinovich¹⁷⁷, J.H. Rawling⁹⁸, M. Raymond³⁵, A.L. Read¹³¹, N.P. Readoff⁵⁶, M. Reale^{65a,65b}, D.M. Rebuzzi^{68a,68b}, A. Redelbach¹⁷⁴, G. Redlinger^{26b}, R. Reece¹⁴³, R.G. Reed^{32c}, K. Reeves⁴², L. Rehnisch¹⁹, J. Reichert¹³⁴, D. Reikher¹⁵⁸, A. Reiss⁹⁷, A. Rej¹⁴⁸, C. Rembser³⁵, H. Ren^{15d}, M. Rescigno^{70a}, S. Resconi^{66a}, E.D. Resseguie¹³⁴, S. Rettie¹⁷², E. Reynolds²¹, O.L. Rezanova^{120b,120a}, P. Reznicek¹⁴⁰, E. Ricci^{73a,73b}, R. Richter¹¹³, S. Richter⁴⁴, E. Richter-Was^{81b}, O. Ricken²⁴, M. Ridel¹³³, P. Rieck¹¹³, C.J. Riegel¹⁷⁹, O. Rifki⁴⁴, M. Rijssenbeek¹⁵², A. Rimoldi^{68a,68b}, M. Rimoldi²⁰, L. Rinaldi^{23b}, G. Ripellino¹⁵¹, B. Ristić⁸⁷, E. Ritsch³⁵, I. Riu¹⁴, J.C. Rivera Vergara^{144a}, F. Rizatdinova¹²⁶, E. Rizvi⁹⁰, C. Rizzi¹⁴, R.T. Roberts⁹⁸, S.H. Robertson^{101,ac}, D. Robinson³¹, J.E.M. Robinson⁴⁴, A. Robson⁵⁵, E. Rocco⁹⁷, C. Roda^{69a,69b}, Y. Rodina⁹⁹, S. Rodriguez Bosca¹⁷¹, A. Rodriguez Perez¹⁴, D. Rodriguez Rodriguez¹⁷¹, A.M. Rodríguez Vera^{165b}, S. Roe³⁵, C.S. Rogan⁵⁷, O. Röhne¹³¹, R. Röhrig¹¹³, C.P.A. Roland⁶³, J. Roloff⁵⁷, A. Romaniouk¹¹⁰, M. Romano^{23b,23a}, N. Rompotis⁸⁸, M. Ronzani¹²², L. Roos¹³³, S. Rosati^{70a}, K. Rosbach⁵⁰, N.-A. Rosien⁵¹, B.J. Rosser¹³⁴, E. Rossi⁴⁴, E. Rossi^{72a,72b}, E. Rossi^{67a,67b}, L.P. Rossi^{53b}, L. Rossini^{66a,66b}, J.H.N. Rosten³¹, R. Rosten¹⁴, M. Rotaru^{28b}, J. Rothberg¹⁴⁵, D. Rousseau¹²⁹, D. Roy^{32c}, A. Rozanov⁹⁹, Y. Rozen¹⁵⁷, X. Ruan^{32c}, F. Rubbo¹⁵⁰, F. Rühr⁵⁰, A. Ruiz-Martinez¹⁷¹, Z. Rurikova⁵⁰, N.A. Rusakovitch⁷⁷, H.L. Russell¹⁰¹, J.P. Rutherford⁷, E.M. Rüttinger^{44,l}, Y.F. Ryabov¹³⁵, M. Rybar³⁸, G. Rybkin¹²⁹, S. Ryu⁶, A. Ryzhov¹²¹, G.F. Rzehorz⁵¹,

P. Sabatini⁵¹, G. Sabato¹¹⁸, S. Sacerdoti¹²⁹, H.F.-W. Sadrozinski¹⁴³, R. Sadykov⁷⁷, F. Safai Tehrani^{70a}, P. Saha¹¹⁹, M. Sahinsoy^{59a}, A. Sahu¹⁷⁹, M. Saimpert⁴⁴, M. Saito¹⁶⁰, T. Saito¹⁶⁰, H. Sakamoto¹⁶⁰, A. Sakharov^{122,am}, D. Salamani⁵², G. Salamanna^{72a,72b}, J.E. Salazar Loyola^{144b}, P.H. Sales De Bruin¹⁶⁹, D. Salihagic^{113,*}, A. Salnikov¹⁵⁰, J. Salt¹⁷¹, D. Salvatore^{40b,40a}, F. Salvatore¹⁵³, A. Salvucci^{61a,61b,61c}, A. Salzburger³⁵, J. Samarati³⁵, D. Sammel⁵⁰, D. Sampsonidis¹⁵⁹, D. Sampsonidou¹⁵⁹, J. Sánchez¹⁷¹, A. Sanchez Pineda^{64a,64c}, H. Sandaker¹³¹, C.O. Sander⁴⁴, M. Sandhoff¹⁷⁹, C. Sandoval²², D.P.C. Sankey¹⁴¹, M. Sannino^{53b,53a}, Y. Sano¹¹⁵, A. Sansoni⁴⁹, C. Santoni³⁷, H. Santos^{137a}, I. Santoyo Castillo¹⁵³, A. Santra¹⁷¹, A. Saponov⁷⁷, J.G. Saraiva^{137a,137d}, O. Sasaki⁷⁹, K. Sato¹⁶⁶, E. Sauvan⁵, P. Savard^{164,av}, N. Savic¹¹³, R. Sawada¹⁶⁰, C. Sawyer¹⁴¹, L. Sawyer^{93,ak}, C. Sbarra^{23b}, A. Sbrizzi^{23a}, T. Scanlon⁹², J. Schaarschmidt¹⁴⁵, P. Schacht¹¹³, B.M. Schachtner¹¹², D. Schaefer³⁶, L. Schaefer¹³⁴, J. Schaeffer⁹⁷, S. Schaepe³⁵, U. Schäfer⁹⁷, A.C. Schaffer¹²⁹, D. Schaile¹¹², R.D. Schamberger¹⁵², N. Scharmberg⁹⁸, V.A. Schegelsky¹³⁵, D. Scheirich¹⁴⁰, F. Schenck¹⁹, M. Schernau¹⁶⁸, C. Schiavi^{53b,53a}, S. Schier¹⁴³, L.K. Schildgen²⁴, Z.M. Schillaci²⁷, E.J. Schioppa³⁵, M. Schioppa^{40b,40a}, K.E. Schleicher⁵⁰, S. Schlenker³⁵, K.R. Schmidt-Sommerfeld¹¹³, K. Schmieden³⁵, C. Schmitt⁹⁷, S. Schmitt⁴⁴, S. Schmitz⁹⁷, J.C. Schmoeckel⁴⁴, U. Schnoor⁵⁰, L. Schoeffel¹⁴², A. Schoening^{59b}, E. Schopf¹³², M. Schott⁹⁷, J.F.P. Schouwenberg¹¹⁷, J. Schovancova³⁵, S. Schramm⁵², A. Schulte⁹⁷, H.-C. Schultz-Coulon^{59a}, M. Schumacher⁵⁰, B.A. Schumm¹⁴³, Ph. Schune¹⁴², A. Schwartzman¹⁵⁰, T.A. Schwarz¹⁰³, Ph. Schwemling¹⁴², R. Schwienhorst¹⁰⁴, A. Sciandra²⁴, G. Sciolla²⁷, M. Scornajenghi^{40b,40a}, F. Scuri^{69a}, F. Scutti¹⁰², L.M. Scyboz¹¹³, C.D. Sebastiani^{70a,70b}, P. Seema¹⁹, S.C. Seidel¹¹⁶, A. Seiden¹⁴³, T. Seiss³⁶, J.M. Seixas^{78b}, G. Sekhniaidze^{67a}, K. Sekhon¹⁰³, S.J. Sekula⁴¹, N. Semprini-Cesari^{23b,23a}, S. Sen⁴⁷, S. Senkin³⁷, C. Serfon¹³¹, L. Serin¹²⁹, L. Serkin^{64a,64b}, M. Sessa^{58a}, H. Severini¹²⁵, F. Sforza¹⁶⁷, A. Sfyrly⁵², E. Shabalina⁵¹, J.D. Shahinian¹⁴³, N.W. Shaikh^{43a,43b}, D. Shaked Renous¹⁷⁷, L.Y. Shan^{15a}, R. Shang¹⁷⁰, J.T. Shank²⁵, M. Shapiro¹⁸, A.S. Sharma¹, A. Sharma¹³², P.B. Shatalov¹⁰⁹, K. Shaw¹⁵³, S.M. Shaw⁹⁸, A. Shcherbakova¹³⁵, Y. Shen¹²⁵, N. Sherafati³³, A.D. Sherman²⁵, P. Sherwood⁹², L. Shi^{155,ar}, S. Shimizu⁷⁹, C.O. Shimmin¹⁸⁰, Y. Shimogama¹⁷⁶, M. Shimojima¹¹⁴, I.P.J. Shipsey¹³², S. Shirabe⁸⁵, M. Shiyakova⁷⁷, J. Shlomi¹⁷⁷, A. Shmeleva¹⁰⁸, D. Shoaleh Saadi¹⁰⁷, M.J. Shochet³⁶, S. Shojaii¹⁰², D.R. Shope¹²⁵, S. Shrestha¹²³, E. Shulga¹¹⁰, P. Sicho¹³⁸, A.M. Sickles¹⁷⁰, P.E. Sidebo¹⁵¹, E. Sideras Haddad^{32c}, O. Sidiropoulou³⁵, A. Sidoti^{23b,23a}, F. Siegert⁴⁶, Dj. Sijacki¹⁶, J. Silva^{137a}, M. Silva Jr.¹⁷⁸, M.V. Silva Oliveira^{78a}, S.B. Silverstein^{43a}, S. Simion¹²⁹, E. Simioni⁹⁷, M. Simon⁹⁷, R. Simoniello⁹⁷, P. Sinervo¹⁶⁴, N.B. Sinev¹²⁸, M. Sioli^{23b,23a}, I. Siral¹⁰³, S.Yu. Sivoklov¹¹¹, J. Sjölin^{43a,43b}, P. Skubic¹²⁵, M. Slater²¹, T. Slavicek¹³⁹, M. Slawinska⁸², K. Sliwa¹⁶⁷, R. Slovak¹⁴⁰, V. Smakhtin¹⁷⁷, B.H. Smart⁵, J. Smiesko^{29a}, N. Smirnov¹¹⁰, S.Yu. Smirnov¹¹⁰, Y. Smirnov¹¹⁰, L.N. Smirnova¹¹¹, O. Smirnova⁹⁴, J.W. Smith⁵¹, M. Smizanska⁸⁷, K. Smolek¹³⁹, A. Smykiewicz⁸², A.A. Snesarev¹⁰⁸, I.M. Snyder¹²⁸, S. Snyder^{26b}, R. Sobie^{173,ac}, A.M. Soffa¹⁶⁸, A. Soffer¹⁵⁸, A. Søgaard⁴⁸, F. Sohns⁵¹, G. Sokhrannyi⁸⁹, C.A. Solans Sanchez³⁵, M. Solar¹³⁹, E.Yu. Soldatov¹¹⁰, U. Soldevila¹⁷¹, A.A. Solodkov¹²¹, A. Soloshenko⁷⁷, O.V. Solovyanov¹²¹, V. Solovyev¹³⁵, P. Sommer¹⁴⁶, H. Son¹⁶⁷, W. Song¹⁴¹, W.Y. Song^{165b}, A. Sopczak¹³⁹, F. Sopkova^{29b}, C.L. Sotiropoulou^{69a,69b}, S. Sottocornola^{68a,68b}, R. Soualah^{64a,64c,i}, A.M. Soukharev^{120b,120a}, D. South⁴⁴, S. Spagnolo^{65a,65b}, M. Spalla¹¹³, M. Spangenberg¹⁷⁵, F. Spanò⁹¹, D. Sperlich¹⁹, T.M. Spieker^{59a}, R. Spighi^{23b}, G. Spigo³⁵, L.A. Spiller¹⁰², D.P. Spiteri⁵⁵, M. Spousta¹⁴⁰, A. Stabile^{66a,66b}, R. Stamen^{59a}, S. Stamm¹⁹, E. Stanecka⁸², R.W. Stanek⁶, C. Stanescu^{72a}, B. Stanislaus¹³², M.M. Stanitzki⁴⁴, B. Stapf¹¹⁸, E.A. Starchenko¹²¹, G.H. Stark¹⁴³, J. Stark⁵⁶, S.H. Stark³⁹, P. Staroba¹³⁸, P. Starovoitov^{59a}, S. Stärz¹⁰¹, R. Staszewski⁸², M. Stegler⁴⁴, P. Steinberg^{26b}, B. Stelzer¹⁴⁹, H.J. Stelzer³⁵, O. Stelzer-Chilton^{165a}, H. Stenzel⁵⁴, T.J. Stevenson¹⁵³, G.A. Stewart³⁵, M.C. Stockton³⁵, G. Stoica^{28b}, P. Stolte⁵¹, S. Stonjek¹¹³, A. Straessner⁴⁶, J. Strandberg¹⁵¹, S. Strandberg^{43a,43b}, M. Strauss¹²⁵, P. Strizenec^{29b}, R. Ströhmer¹⁷⁴, D.M. Strom¹²⁸, R. Stroynowski⁴¹, A. Strubig⁴⁸, S.A. Stucci^{26b}, B. Stugu¹⁷, J. Stupak¹²⁵, N.A. Styles⁴⁴, D. Su¹⁵⁰, J. Su¹³⁶, S. Suchek^{59a}, Y. Sugaya¹³⁰, M. Suk¹³⁹, V.V. Sulin¹⁰⁸, M.J. Sullivan⁸⁸, D.M.S. Sultan⁵², S. Sultansoy^{4c}, T. Sumida⁸³, S. Sun¹⁰³, X. Sun³, K. Suruliz¹⁵³, C.J.E. Suster¹⁵⁴, M.R. Sutton¹⁵³, S. Suzuki⁷⁹, M. Svatos¹³⁸, M. Swiatlowski³⁶, S.P. Swift², A. Sydorenko⁹⁷, I. Sykora^{29a}, M. Sykora¹⁴⁰, T. Sykora¹⁴⁰, D. Ta⁹⁷, K. Tackmann^{44,z}, J. Taenzer¹⁵⁸, A. Taffard¹⁶⁸, R. Tafirout^{165a}, E. Tahirovic⁹⁰, N. Taiblum¹⁵⁸, H. Takai^{26b}, R. Takashima⁸⁴, E.H. Takasugi¹¹³, K. Takeda⁸⁰, T. Takeshita¹⁴⁷, Y. Takubo⁷⁹, M. Talby⁹⁹, A.A. Talyshv^{120b,120a}, J. Tanaka¹⁶⁰, M. Tanaka¹⁶², R. Tanaka¹²⁹, B.B. Tannenwald¹²³,

S. Tapia Araya¹⁷⁰, S. Tapprogge⁹⁷, A. Tarek Abouelfadl Mohamed¹³³, S. Tarem¹⁵⁷, G. Tarna^{28b,e}, G.F. Tartarelli^{66a}, P. Tas¹⁴⁰, M. Tasevsky¹³⁸, T. Tashiro⁸³, E. Tassi^{40b,40a}, A. Tavares Delgado^{137a,137b}, Y. Tayalati^{34e}, A.J. Taylor⁴⁸, G.N. Taylor¹⁰², P.T.E. Taylor¹⁰², W. Taylor^{165b}, A.S. Tee⁸⁷, R. Teixeira De Lima¹⁵⁰, P. Teixeira-Dias⁹¹, H. Ten Kate³⁵, J.J. Teoh¹¹⁸, S. Terada⁷⁹, K. Terashi¹⁶⁰, J. Terron⁹⁶, S. Terzo¹⁴, M. Testa⁴⁹, R.J. Teuscher^{164,ac}, S.J. Thais¹⁸⁰, T. Theveneaux-Pelzer⁴⁴, F. Thiele³⁹, D.W. Thomas⁹¹, J.P. Thomas²¹, A.S. Thompson⁵⁵, P.D. Thompson²¹, L.A. Thomsen¹⁸⁰, E. Thomson¹³⁴, Y. Tian³⁸, R.E. Ticse Torres⁵¹, V.O. Tikhomirov^{108,ao}, Yu.A. Tikhonov^{120b,120a}, S. Timoshenko¹¹⁰, P. Tipton¹⁸⁰, S. Tisserant⁹⁹, K. Todome¹⁶², S. Todorova-Nova⁵, S. Todt⁴⁶, J. Tojo⁸⁵, S. Tokár^{29a}, K. Tokushuku⁷⁹, E. Tolley¹²³, K.G. Tomiwa^{32c}, M. Tomoto¹¹⁵, L. Tompkins^{150,q}, K. Toms¹¹⁶, B. Tong⁵⁷, P. Tornambe⁵⁰, E. Torrence¹²⁸, H. Torres⁴⁶, E. Torró Pastor¹⁴⁵, C. Toscirci¹³², J. Toth^{99,ab}, F. Touchard⁹⁹, D.R. Tovey¹⁴⁶, C.J. Treado¹²², T. Trefzger¹⁷⁴, F. Tresoldi¹⁵³, A. Tricoli^{26b}, I.M. Trigger^{165a}, S. Trincaz-Duvoid¹³³, W. Trischuk¹⁶⁴, B. Trocmé⁵⁶, A. Trofymov¹²⁹, C. Troncon^{66a}, M. Trovatelli¹⁷³, F. Trovato¹⁵³, L. Truong^{32b}, M. Trzebinski⁸², A. Trzupek⁸², F. Tsai⁴⁴, J.C.-L. Tseng¹³², P.V. Tsiarshka^{105,ai}, A. Tsigotis¹⁵⁹, N. Tsirintanis⁹, V. Tsiskaridze¹⁵², E.G. Tskhadadze^{156a}, I.I. Tsukerman¹⁰⁹, V. Tsulaia¹⁸, S. Tsuno⁷⁹, D. Tsybychev^{152,163}, Y. Tu^{61b}, A. Tudorache^{28b}, V. Tudorache^{28b}, T.T. Tulbure^{28a}, A.N. Tuna⁵⁷, S. Turchikhin⁷⁷, D. Turgeman¹⁷⁷, I. Turk Cakir^{4b,t}, R.J. Turner²¹, R.T. Turra^{66a}, P.M. Tuts³⁸, S. Tzamarias¹⁵⁹, E. Tzovara⁹⁷, G. Ucchielli⁴⁵, I. Ueda⁷⁹, M. Ughetto^{43a,43b}, F. Ukegawa¹⁶⁶, G. Unal³⁵, A. Undrus^{26b}, G. Unel¹⁶⁸, F.C. Ungaro¹⁰², Y. Unno⁷⁹, K. Uno¹⁶⁰, J. Urban^{29b}, P. Urquijo¹⁰², G. Usai⁸, J. Usui⁷⁹, L. Vacavant⁹⁹, V. Vacek¹³⁹, B. Vachon¹⁰¹, K.O.H. Vadla¹³¹, A. Vaidya⁹², C. Valderanis¹¹², E. Valdes Santurio^{43a,43b}, M. Valente⁵², S. Valentini^{23b,23a}, A. Valero¹⁷¹, L. Valéry⁴⁴, R.A. Vallance²¹, A. Vallier⁵, J.A. Valls Ferrer¹⁷¹, T.R. Van Daalen¹⁴, H. Van der Graaf¹¹⁸, P. Van Gemmeren⁶, I. Van Vulpen¹¹⁸, M. Vanadia^{71a,71b}, W. Vandelli³⁵, A. Vaniachine¹⁶³, P. Vankov¹¹⁸, R. Vari^{70a}, E.W. Varnes⁷, C. Varni^{53b,53a}, T. Varol⁴¹, D. Varouchas¹²⁹, K.E. Varvell¹⁵⁴, G.A. Vasquez^{144b}, J.G. Vasquez¹⁸⁰, F. Vazeille³⁷, D. Vazquez Furelos¹⁴, T. Vazquez Schroeder³⁵, J. Veatch⁵¹, V. Vecchio^{72a,72b}, L.M. Veloce¹⁶⁴, F. Veloso^{137a,137c}, S. Veneziano^{70a}, A. Ventura^{65a,65b}, N. Venturi³⁵, V. Vercesi^{68a}, M. Verducci^{72a,72b}, C.M. Vergel Infante⁷⁶, C. Vergis²⁴, W. Verkerke¹¹⁸, A.T. Vermeulen¹¹⁸, J.C. Vermeulen¹¹⁸, M.C. Vetterli^{149,av}, N. Viaux Maira^{144b}, M. Vicente Barreto Pinto⁵², I. Vichou^{170,*}, T. Vickey¹⁴⁶, O.E. Vickey Boeriu¹⁴⁶, G.H.A. Viehhauser¹³², S. Viel¹⁸, L. Vigani¹³², M. Villa^{23b,23a}, M. Villaplana Perez^{66a,66b}, E. Vilucchi⁴⁹, M.G. Vincet³³, V.B. Vinogradov⁷⁷, A. Vishwakarma⁴⁴, C. Vittori^{23b,23a}, I. Vivarelli¹⁵³, S. Vlachos¹⁰, M. Vogel¹⁷⁹, P. Vokac¹³⁹, G. Volpi¹⁴, S.E. von Buddenbrock^{32c}, E. Von Toerne²⁴, V. Vorobel¹⁴⁰, K. Vorobev¹¹⁰, M. Vos¹⁷¹, J.H. Vosseveld⁸⁸, N. Vranjes¹⁶, M. Vranjes Milosavljevic¹⁶, V. Vrba¹³⁹, M. Vreeswijk¹¹⁸, T. Šfiligoj⁸⁹, R. Vuillermet³⁵, I. Vukotic³⁶, T. Ženiš^{29a}, L. Živković¹⁶, P. Wagner²⁴, W. Wagner¹⁷⁹, J. Wagner-Kuhr¹¹², H. Wahlberg⁸⁶, S. Wahrenmund⁴⁶, K. Wakamiya⁸⁰, V.M. Walbrecht¹¹³, J. Walder⁸⁷, R. Walker¹¹², S.D. Walker⁹¹, W. Walkowiak¹⁴⁸, V. Wallangen^{43a,43b}, A.M. Wang⁵⁷, C. Wang^{58b}, F. Wang¹⁷⁸, H. Wang¹⁸, H. Wang³, J. Wang¹⁵⁴, J. Wang^{59b}, P. Wang⁴¹, Q. Wang¹²⁵, R.-J. Wang¹³³, R. Wang^{58a}, R. Wang⁶, S.M. Wang¹⁵⁵, W.T. Wang^{58a}, W. Wang^{15c,ad}, W.X. Wang^{58a,ad}, Y. Wang^{58a,al}, Z. Wang^{58c}, C. Wanotayaroj⁴⁴, A. Warburton¹⁰¹, C.P. Ward³¹, D.R. Wardrope⁹², A. Washbrook⁴⁸, P.M. Watkins²¹, A.T. Watson²¹, M.F. Watson²¹, G. Watts¹⁴⁵, S. Watts⁹⁸, B.M. Waugh⁹², A.F. Webb¹¹, S. Webb⁹⁷, C. Weber¹⁸⁰, M.S. Weber²⁰, S.A. Weber³³, S.M. Weber^{59a}, A.R. Weidberg¹³², J. Weingarten⁴⁵, M. Weirich⁹⁷, C. Weiser⁵⁰, P.S. Wells³⁵, T. Wenaus^{26b}, T. Wengler³⁵, S. Wenig³⁵, N. Wermes²⁴, M.D. Werner⁷⁶, P. Werner³⁵, M. Wessels^{59a}, T.D. Weston²⁰, K. Whalen¹²⁸, N.L. Whallon¹⁴⁵, A.M. Wharton⁸⁷, A.S. White¹⁰³, A. White⁸, M.J. White¹, R. White^{144b}, D. Whiteson¹⁶⁸, B.W. Whitmore⁸⁷, F.J. Wickens¹⁴¹, W. Wiedenmann¹⁷⁸, M. Wielers¹⁴¹, C. Wiglesworth³⁹, L.A.M. Wiik-Fuchs⁵⁰, F. Wilk⁹⁸, H.G. Wilkens³⁵, L.J. Wilkins⁹¹, H.H. Williams¹³⁴, S. Williams³¹, C. Willis¹⁰⁴, S. Willocq¹⁰⁰, J.A. Wilson²¹, I. Wingerter-Seez⁵, E. Winkels¹⁵³, F. Winklmeier¹²⁸, O.J. Winston¹⁵³, B.T. Winter⁵⁰, M. Wittgen¹⁵⁰, M. Wobisch⁹³, A. Wolf⁹⁷, T.M.H. Wolf¹¹⁸, R. Wolff⁹⁹, J. Wollrath⁵⁰, M.W. Wolter⁸², H. Wolters^{137a,137c}, V.W.S. Wong¹⁷², N.L. Woods¹⁴³, S.D. Worm²¹, B.K. Wosiek⁸², K.W. Woźniak⁸², K. Wraight⁵⁵, M. Wu³⁶, S.L. Wu¹⁷⁸, X. Wu⁵², Y. Wu^{58a}, T.R. Wyatt⁹⁸, B.M. Wynne⁴⁸, S. Xella³⁹, Z. Xi¹⁰³, L. Xia¹⁷⁵, D. Xu^{15a}, H. Xu^{58a,e}, L. Xu^{26b}, T. Xu¹⁴², W. Xu¹⁰³, Z. Xu¹⁵⁰, B. Yabsley¹⁵⁴, S. Yacoob^{32a}, K. Yajima¹³⁰, D.P. Yallup⁹², D. Yamaguchi¹⁶², Y. Yamaguchi¹⁶², A. Yamamoto⁷⁹, T. Yamanaka¹⁶⁰, F. Yamane⁸⁰, M. Yamatani¹⁶⁰, T. Yamazaki¹⁶⁰, Y. Yamazaki⁸⁰, Z. Yan²⁵, H.J. Yang^{58c,58d}, H.T. Yang¹⁸, S. Yang⁷⁵,

Y. Yang¹⁶⁰, Z. Yang¹⁷, W.-M. Yao¹⁸, Y.C. Yap⁴⁴, Y. Yasu⁷⁹, E. Yatsenko^{58c,58d}, J. Ye⁴¹, S. Ye^{26b},
 I. Yeletsikh⁷⁷, E. Yigitbasi²⁵, E. Yildirim⁹⁷, K. Yorita¹⁷⁶, K. Yoshihara¹³⁴, C.J.S. Young³⁵, C. Young¹⁵⁰,
 J. Yu⁸, J. Yu⁷⁶, X. Yue^{59a}, S.P.Y. Yuen²⁴, B. Zabinski⁸², G. Zacharis¹⁰, E. Zaffaroni⁵², R. Zaidan¹⁴,
 A.M. Zaitsev^{121,an}, T. Zakareishvili^{156b}, N. Zakharchuk³³, S. Zambito⁵⁷, D. Zanzi³⁵, D.R. Zaripovas⁵⁵,
 S.V. Zeißner⁴⁵, C. Zeitnitz¹⁷⁹, G. Zemaityte¹³², J.C. Zeng¹⁷⁰, Q. Zeng¹⁵⁰, O. Zenin¹²¹, D. Zerwas¹²⁹,
 M. Zgubić¹³², D.F. Zhang^{58b}, D. Zhang¹⁰³, F. Zhang¹⁷⁸, G. Zhang^{58a}, G. Zhang^{15b}, H. Zhang^{15c},
 J. Zhang⁶, L. Zhang^{15c}, L. Zhang^{58a}, M. Zhang¹⁷⁰, P. Zhang^{15c}, R. Zhang^{58a}, R. Zhang²⁴, X. Zhang^{58b},
 Y. Zhang^{15d}, Z. Zhang¹²⁹, P. Zhao⁴⁷, Y. Zhao^{58b,129,aj}, Z. Zhao^{58a}, A. Zhemchugov⁷⁷, Z. Zheng¹⁰³,
 D. Zhong¹⁷⁰, B. Zhou¹⁰³, C. Zhou¹⁷⁸, M.S. Zhou^{15d}, M. Zhou¹⁵², N. Zhou^{58c}, Y. Zhou⁷, C.G. Zhu^{58b},
 H.L. Zhu^{58a}, H. Zhu^{15a}, J. Zhu¹⁰³, Y. Zhu^{58a}, X. Zhuang^{15a}, K. Zhukov¹⁰⁸, V. Zhulanov^{120b,120a},
 A. Zibell¹⁷⁴, D. Zieminska⁶³, N.I. Zimine⁷⁷, S. Zimmermann⁵⁰, Z. Zinonos¹¹³, M. Ziolkowski¹⁴⁸,
 G. Zobernig¹⁷⁸, A. Zoccoli^{23b,23a}, K. Zoch⁵¹, T.G. Zorbas¹⁴⁶, R. Zou³⁶, M. Zur Nedden¹⁹, L. Zwalinski³⁵

¹ Department of Physics, University of Adelaide, Adelaide, Australia

² Physics Department, SUNY Albany, Albany, NY, United States of America

³ Department of Physics, University of Alberta, Edmonton, AB, Canada

⁴ (a) Department of Physics, Ankara University, Ankara; (b) Istanbul Aydin University, Istanbul; (c) Division of Physics, TOBB University of Economics and Technology, Ankara, Turkey

⁵ LAPP, Université Grenoble Alpes, Université Savoie Mont Blanc, CNRS/IN2P3, Annecy, France

⁶ High Energy Physics Division, Argonne National Laboratory, Argonne, IL, United States of America

⁷ Department of Physics, University of Arizona, Tucson, AZ, United States of America

⁸ Department of Physics, University of Texas at Arlington, Arlington, TX, United States of America

⁹ Physics Department, National and Kapodistrian University of Athens, Athens, Greece

¹⁰ Physics Department, National Technical University of Athens, Zografou, Greece

¹¹ Department of Physics, University of Texas at Austin, Austin, TX, United States of America

¹² (a) Bahcesehir University, Faculty of Engineering and Natural Sciences, Istanbul; (b) Istanbul Bilgi University, Faculty of Engineering and Natural Sciences, Istanbul; (c) Department of Physics, Bogazici University, Istanbul; (d) Department of Physics Engineering, Gaziantep University, Gaziantep, Turkey

¹³ Institute of Physics, Azerbaijan Academy of Sciences, Baku, Azerbaijan

¹⁴ Institut de Física d'Altes Energies (IFAE), Barcelona Institute of Science and Technology, Barcelona, Spain

¹⁵ (a) Institute of High Energy Physics, Chinese Academy of Sciences, Beijing; (b) Physics Department, Tsinghua University, Beijing; (c) Department of Physics, Nanjing University, Nanjing;

(d) University of Chinese Academy of Science (UCAS), Beijing, China

¹⁶ Institute of Physics, University of Belgrade, Belgrade, Serbia

¹⁷ Department for Physics and Technology, University of Bergen, Bergen, Norway

¹⁸ Physics Division, Lawrence Berkeley National Laboratory and University of California, Berkeley, CA, United States of America

¹⁹ Institut für Physik, Humboldt Universität zu Berlin, Berlin, Germany

²⁰ Albert Einstein Center for Fundamental Physics and Laboratory for High Energy Physics, University of Bern, Bern, Switzerland

²¹ School of Physics and Astronomy, University of Birmingham, Birmingham, United Kingdom

²² Centro de Investigaciones, Universidad Antonio Nariño, Bogotá, Colombia

²³ (a) INFN Bologna and Università di Bologna, Dipartimento di Fisica; (b) INFN Sezione di Bologna, Italy

²⁴ Physikalisches Institut, Universität Bonn, Bonn, Germany

²⁵ Department of Physics, Boston University, Boston, MA, United States of America

²⁶ (a) University of Colorado Boulder, Department of Physics, CO; (b) Physics Department, Brookhaven National Laboratory, Upton, NY, United States of America

²⁷ Department of Physics, Brandeis University, Waltham, MA, United States of America

²⁸ (a) Transilvania University of Brasov, Brasov; (b) Horia Hulubei National Institute of Physics and Nuclear Engineering, Bucharest; (c) Department of Physics, Alexandru Ioan Cuza

University of Iasi, Iasi; (d) National Institute for Research and Development of Isotopic and Molecular Technologies, Physics Department, Cluj-Napoca; (e) University Politehnica Bucharest, Bucharest; (f) West University in Timisoara, Timisoara, Romania

²⁹ (a) Faculty of Mathematics, Physics and Informatics, Comenius University, Bratislava; (b) Department of Subnuclear Physics, Institute of Experimental Physics of the Slovak Academy of Sciences, Kosice, Slovak Republic

³⁰ Departamento de Física, Universidad de Buenos Aires, Buenos Aires, Argentina

³¹ Cavendish Laboratory, University of Cambridge, Cambridge, United Kingdom

³² (a) Department of Physics, University of Cape Town, Cape Town; (b) Department of Mechanical Engineering Science, University of Johannesburg, Johannesburg; (c) School of Physics, University of the Witwatersrand, Johannesburg, South Africa

³³ Department of Physics, Carleton University, Ottawa, ON, Canada

³⁴ (a) Faculté des Sciences Ain Chock, Réseau Universitaire de Physique des Hautes Energies – Université Hassan II, Casablanca; (b) Centre National de l'Energie des Sciences Techniques Nucleaires (CNESTEN), Rabat; (c) Faculté des Sciences Semlalia, Université Cadi Ayyad, LPHEA, Marrakech; (d) Faculté des Sciences, Université Mohamed Premier and LPTPM, Oujda;

(e) Faculté des sciences, Université Mohammed V, Rabat, Morocco

³⁵ CERN, Geneva, Switzerland

³⁶ Enrico Fermi Institute, University of Chicago, Chicago, IL, United States of America

³⁷ LPC, Université Clermont Auvergne, CNRS/IN2P3, Clermont-Ferrand, France

³⁸ Nevis Laboratory, Columbia University, Irvington, NY, United States of America

³⁹ Niels Bohr Institute, University of Copenhagen, Copenhagen, Denmark

⁴⁰ (a) Dipartimento di Fisica, Università della Calabria, Rende; (b) INFN Gruppo Collegato di Cosenza, Laboratori Nazionali di Frascati, Italy

⁴¹ Physics Department, Southern Methodist University, Dallas, TX, United States of America

⁴² Physics Department, University of Texas at Dallas, Richardson, TX, United States of America

⁴³ (a) Department of Physics, Stockholm University; (b) Oskar Klein Centre, Stockholm, Sweden

⁴⁴ Deutsches Elektronen-Synchrotron DESY, Hamburg and Zeuthen, Germany

⁴⁵ Lehrstuhl für Experimentelle Physik IV, Technische Universität Dortmund, Dortmund, Germany

⁴⁶ Institut für Kern- und Teilchenphysik, Technische Universität Dresden, Dresden, Germany

⁴⁷ Department of Physics, Duke University, Durham, NC, United States of America

⁴⁸ SUPA – School of Physics and Astronomy, University of Edinburgh, Edinburgh, United Kingdom

⁴⁹ INFN e Laboratori Nazionali di Frascati, Frascati, Italy

⁵⁰ Physikalisches Institut, Albert-Ludwigs-Universität Freiburg, Freiburg, Germany

⁵¹ II. Physikalisches Institut, Georg-August-Universität Göttingen, Göttingen, Germany

⁵² Département de Physique Nucléaire et Corpusculaire, Université de Genève, Genève, Switzerland

- ⁵³ (a) Dipartimento di Fisica, Università di Genova, Genova; (b) INFN Sezione di Genova, Italy
- ⁵⁴ II. Physikalisches Institut, Justus-Liebig-Universität Giessen, Giessen, Germany
- ⁵⁵ SUPA – School of Physics and Astronomy, University of Glasgow, Glasgow, United Kingdom
- ⁵⁶ LPSC, Université Grenoble Alpes, CNRS/IN2P3, Grenoble INP, Grenoble, France
- ⁵⁷ Laboratory for Particle Physics and Cosmology, Harvard University, Cambridge, MA, United States of America
- ⁵⁸ (a) Department of Modern Physics and State Key Laboratory of Particle Detection and Electronics, University of Science and Technology of China, Hefei; (b) Institute of Frontier and Interdisciplinary Science and Key Laboratory of Particle Physics and Particle Irradiation (MOE), Shandong University, Qingdao; (c) School of Physics and Astronomy, Shanghai Jiao Tong University, KLPPAC-MoE, SKLPPC, Shanghai; (d) Tsung-Dao Lee Institute, Shanghai, China
- ⁵⁹ (a) Kirchhoff-Institut für Physik, Ruprecht-Karls-Universität Heidelberg, Heidelberg; (b) Physikalisches Institut, Ruprecht-Karls-Universität Heidelberg, Heidelberg, Germany
- ⁶⁰ Faculty of Applied Information Science, Hiroshima Institute of Technology, Hiroshima, Japan
- ⁶¹ (a) Department of Physics, Chinese University of Hong Kong, Shatin, N.T., Hong Kong; (b) Department of Physics, University of Hong Kong, Hong Kong; (c) Department of Physics and Institute for Advanced Study, Hong Kong University of Science and Technology, Clear Water Bay, Kowloon, Hong Kong, China
- ⁶² Department of Physics, National Tsing Hua University, Hsinchu, Taiwan
- ⁶³ Department of Physics, Indiana University, Bloomington, IN, United States of America
- ⁶⁴ (a) INFN Gruppo Collegato di Udine, Sezione di Trieste, Udine; (b) ICTP, Trieste; (c) Dipartimento Politecnico di Ingegneria e Architettura, Università di Udine, Udine, Italy
- ⁶⁵ (a) INFN Sezione di Lecce; (b) Dipartimento di Matematica e Fisica, Università del Salento, Lecce, Italy
- ⁶⁶ (a) INFN Sezione di Milano; (b) Dipartimento di Fisica, Università di Milano, Milano, Italy
- ⁶⁷ (a) INFN Sezione di Napoli; (b) Dipartimento di Fisica, Università di Napoli, Napoli, Italy
- ⁶⁸ (a) INFN Sezione di Pavia; (b) Dipartimento di Fisica, Università di Pavia, Pavia, Italy
- ⁶⁹ (a) INFN Sezione di Pisa; (b) Dipartimento di Fisica E. Fermi, Università di Pisa, Pisa, Italy
- ⁷⁰ (a) INFN Sezione di Roma; (b) Dipartimento di Fisica, Sapienza Università di Roma, Roma, Italy
- ⁷¹ (a) INFN Sezione di Roma Tor Vergata; (b) Dipartimento di Fisica, Università di Roma Tor Vergata, Roma, Italy
- ⁷² (a) INFN Sezione di Roma Tre; (b) Dipartimento di Matematica e Fisica, Università Roma Tre, Roma, Italy
- ⁷³ (a) INFN-TIFPA; (b) Università degli Studi di Trento, Trento, Italy
- ⁷⁴ Institut für Astro- und Teilchenphysik, Leopold-Franzens-Universität, Innsbruck, Austria
- ⁷⁵ University of Iowa, Iowa City, IA, United States of America
- ⁷⁶ Department of Physics and Astronomy, Iowa State University, Ames, IA, United States of America
- ⁷⁷ Joint Institute for Nuclear Research, Dubna, Russia
- ⁷⁸ (a) Departamento de Engenharia Elétrica, Universidade Federal de Juiz de Fora (UFJF), Juiz de Fora; (b) Universidade Federal do Rio De Janeiro COPPE/EE/IF, Rio de Janeiro; (c) Universidade Federal de São João del Rei (UFSJ), São João del Rei; (d) Instituto de Física, Universidade de São Paulo, São Paulo, Brazil
- ⁷⁹ KEK, High Energy Accelerator Research Organization, Tsukuba, Japan
- ⁸⁰ Graduate School of Science, Kobe University, Kobe, Japan
- ⁸¹ (a) AGH University of Science and Technology, Faculty of Physics and Applied Computer Science, Krakow; (b) Marian Smoluchowski Institute of Physics, Jagiellonian University, Krakow, Poland
- ⁸² Institute of Nuclear Physics Polish Academy of Sciences, Krakow, Poland
- ⁸³ Faculty of Science, Kyoto University, Kyoto, Japan
- ⁸⁴ Kyoto University of Education, Kyoto, Japan
- ⁸⁵ Research Center for Advanced Particle Physics and Department of Physics, Kyushu University, Fukuoka, Japan
- ⁸⁶ Instituto de Física La Plata, Universidad Nacional de La Plata and CONICET, La Plata, Argentina
- ⁸⁷ Physics Department, Lancaster University, Lancaster, United Kingdom
- ⁸⁸ Oliver Lodge Laboratory, University of Liverpool, Liverpool, United Kingdom
- ⁸⁹ Department of Experimental Particle Physics, Jozef Stefan Institute and Department of Physics, University of Ljubljana, Ljubljana, Slovenia
- ⁹⁰ School of Physics and Astronomy, Queen Mary University of London, London, United Kingdom
- ⁹¹ Department of Physics, Royal Holloway University of London, Egham, United Kingdom
- ⁹² Department of Physics and Astronomy, University College London, London, United Kingdom
- ⁹³ Louisiana Tech University, Ruston, LA, United States of America
- ⁹⁴ Fysiska institutionen, Lunds universitet, Lund, Sweden
- ⁹⁵ Centre de Calcul de l'Institut National de Physique Nucléaire et de Physique des Particules (IN2P3), Villeurbanne, France
- ⁹⁶ Departamento de Física Teórica C-15 and CIAFF, Universidad Autónoma de Madrid, Madrid, Spain
- ⁹⁷ Institut für Physik, Universität Mainz, Mainz, Germany
- ⁹⁸ School of Physics and Astronomy, University of Manchester, Manchester, United Kingdom
- ⁹⁹ CPPM, Aix-Marseille Université, CNRS/IN2P3, Marseille, France
- ¹⁰⁰ Department of Physics, University of Massachusetts, Amherst, MA, United States of America
- ¹⁰¹ Department of Physics, McGill University, Montreal, QC, Canada
- ¹⁰² School of Physics, University of Melbourne, Victoria, Australia
- ¹⁰³ Department of Physics, University of Michigan, Ann Arbor, MI, United States of America
- ¹⁰⁴ Department of Physics and Astronomy, Michigan State University, East Lansing, MI, United States of America
- ¹⁰⁵ B.I. Stepanov Institute of Physics, National Academy of Sciences of Belarus, Minsk, Belarus
- ¹⁰⁶ Research Institute for Nuclear Problems of Byelorussian State University, Minsk, Belarus
- ¹⁰⁷ Group of Particle Physics, University of Montreal, Montreal, QC, Canada
- ¹⁰⁸ P.N. Lebedev Physical Institute of the Russian Academy of Sciences, Moscow, Russia
- ¹⁰⁹ Institute for Theoretical and Experimental Physics of the National Research Centre Kurchatov Institute, Moscow, Russia
- ¹¹⁰ National Research Nuclear University MEPhI, Moscow, Russia
- ¹¹¹ D.V. Skobeltsyn Institute of Nuclear Physics, M.V. Lomonosov Moscow State University, Moscow, Russia
- ¹¹² Fakultät für Physik, Ludwig-Maximilians-Universität München, München, Germany
- ¹¹³ Max-Planck-Institut für Physik (Werner-Heisenberg-Institut), München, Germany
- ¹¹⁴ Nagasaki Institute of Applied Science, Nagasaki, Japan
- ¹¹⁵ Graduate School of Science and Kobayashi-Maskawa Institute, Nagoya University, Nagoya, Japan
- ¹¹⁶ Department of Physics and Astronomy, University of New Mexico, Albuquerque, NM, United States of America
- ¹¹⁷ Institute for Mathematics, Astrophysics and Particle Physics, Radboud University Nijmegen/Nikhef, Nijmegen, Netherlands
- ¹¹⁸ Nikhef National Institute for Subatomic Physics and University of Amsterdam, Amsterdam, Netherlands
- ¹¹⁹ Department of Physics, Northern Illinois University, DeKalb, IL, United States of America
- ¹²⁰ (a) Budker Institute of Nuclear Physics and NSU, SB RAS, Novosibirsk; (b) Novosibirsk State University Novosibirsk, Russia
- ¹²¹ Institute for High Energy Physics of the National Research Centre Kurchatov Institute, Protvino, Russia
- ¹²² Department of Physics, New York University, New York, NY, United States of America
- ¹²³ Ohio State University, Columbus, OH, United States of America
- ¹²⁴ Faculty of Science, Okayama University, Okayama, Japan
- ¹²⁵ Homer L. Dodge Department of Physics and Astronomy, University of Oklahoma, Norman, OK, United States of America
- ¹²⁶ Department of Physics, Oklahoma State University, Stillwater, OK, United States of America

- ¹²⁷ Palacký University, RCPTM, Joint Laboratory of Optics, Olomouc, Czech Republic
¹²⁸ Center for High Energy Physics, University of Oregon, Eugene, OR, United States of America
¹²⁹ LAL, Université Paris-Sud, CNRS/IN2P3, Université Paris-Saclay, Orsay, France
¹³⁰ Graduate School of Science, Osaka University, Osaka, Japan
¹³¹ Department of Physics, University of Oslo, Oslo, Norway
¹³² Department of Physics, Oxford University, Oxford, United Kingdom
¹³³ LPNHE, Sorbonne Université, Paris Diderot Sorbonne Paris Cité, CNRS/IN2P3, Paris, France
¹³⁴ Department of Physics, University of Pennsylvania, Philadelphia, PA, United States of America
¹³⁵ Konstantinov Nuclear Physics Institute of National Research Centre "Kurchatov Institute", PNPI, St. Petersburg, Russia
¹³⁶ Department of Physics and Astronomy, University of Pittsburgh, Pittsburgh, PA, United States of America
¹³⁷ ^(a) Laboratório de Instrumentação e Física Experimental de Partículas – LIP; ^(b) Departamento de Física, Faculdade de Ciências, Universidade de Lisboa, Lisboa; ^(c) Departamento de Física, Universidade de Coimbra, Coimbra; ^(d) Centro de Física Nuclear da Universidade de Lisboa, Lisboa; ^(e) Departamento de Física, Universidade do Minho, Braga; ^(f) Universidad de Granada, Granada (Spain); ^(g) Dep. Física and CEFITEC de Faculdade de Ciências e Tecnologia, Universidade Nova de Lisboa, Caparica, Portugal
¹³⁸ Institute of Physics of the Czech Academy of Sciences, Prague, Czech Republic
¹³⁹ Czech Technical University in Prague, Prague, Czech Republic
¹⁴⁰ Charles University, Faculty of Mathematics and Physics, Prague, Czech Republic
¹⁴¹ Particle Physics Department, Rutherford Appleton Laboratory, Didcot, United Kingdom
¹⁴² IRFU, CEA, Université Paris-Saclay, Gif-sur-Yvette, France
¹⁴³ Santa Cruz Institute for Particle Physics, University of California Santa Cruz, Santa Cruz, CA, United States of America
¹⁴⁴ ^(a) Departamento de Física, Pontificia Universidad Católica de Chile, Santiago; ^(b) Departamento de Física, Universidad Técnica Federico Santa María, Valparaíso, Chile
¹⁴⁵ Department of Physics, University of Washington, Seattle, WA, United States of America
¹⁴⁶ Department of Physics and Astronomy, University of Sheffield, Sheffield, United Kingdom
¹⁴⁷ Department of Physics, Shinshu University, Nagano, Japan
¹⁴⁸ Department Physik, Universität Siegen, Siegen, Germany
¹⁴⁹ Department of Physics, Simon Fraser University, Burnaby, BC, Canada
¹⁵⁰ SLAC National Accelerator Laboratory, Stanford, CA, United States of America
¹⁵¹ Physics Department, Royal Institute of Technology, Stockholm, Sweden
¹⁵² Departments of Physics and Astronomy, Stony Brook University, Stony Brook, NY, United States of America
¹⁵³ Department of Physics and Astronomy, University of Sussex, Brighton, United Kingdom
¹⁵⁴ School of Physics, University of Sydney, Sydney, Australia
¹⁵⁵ Institute of Physics, Academia Sinica, Taipei, Taiwan
¹⁵⁶ ^(a) E. Andronikashvili Institute of Physics, Iv. Javakishvili Tbilisi State University, Tbilisi; ^(b) High Energy Physics Institute, Tbilisi State University, Tbilisi, Georgia
¹⁵⁷ Department of Physics, Technion, Israel Institute of Technology, Haifa, Israel
¹⁵⁸ Raymond and Beverly Sackler School of Physics and Astronomy, Tel Aviv University, Tel Aviv, Israel
¹⁵⁹ Department of Physics, Aristotle University of Thessaloniki, Thessaloniki, Greece
¹⁶⁰ International Center for Elementary Particle Physics and Department of Physics, University of Tokyo, Tokyo, Japan
¹⁶¹ Graduate School of Science and Technology, Tokyo Metropolitan University, Tokyo, Japan
¹⁶² Department of Physics, Tokyo Institute of Technology, Tokyo, Japan
¹⁶³ Tomsk State University, Tomsk, Russia
¹⁶⁴ Department of Physics, University of Toronto, Toronto, ON, Canada
¹⁶⁵ ^(a) TRIUMF, Vancouver, BC; ^(b) Department of Physics and Astronomy, York University, Toronto, ON, Canada
¹⁶⁶ Division of Physics and Tomonaga Center for the History of the Universe, Faculty of Pure and Applied Sciences, University of Tsukuba, Tsukuba, Japan
¹⁶⁷ Department of Physics and Astronomy, Tufts University, Medford, MA, United States of America
¹⁶⁸ Department of Physics and Astronomy, University of California Irvine, Irvine, CA, United States of America
¹⁶⁹ Department of Physics and Astronomy, University of Uppsala, Uppsala, Sweden
¹⁷⁰ Department of Physics, University of Illinois, Urbana, IL, United States of America
¹⁷¹ Instituto de Física Corpuscular (IFIC), Centro Mixto Universidad de Valencia – CSIC, Valencia, Spain
¹⁷² Department of Physics, University of British Columbia, Vancouver, BC, Canada
¹⁷³ Department of Physics and Astronomy, University of Victoria, Victoria, BC, Canada
¹⁷⁴ Fakultät für Physik und Astronomie, Julius-Maximilians-Universität Würzburg, Würzburg, Germany
¹⁷⁵ Department of Physics, University of Warwick, Coventry, United Kingdom
¹⁷⁶ Waseda University, Tokyo, Japan
¹⁷⁷ Department of Particle Physics, Weizmann Institute of Science, Rehovot, Israel
¹⁷⁸ Department of Physics, University of Wisconsin, Madison, WI, United States of America
¹⁷⁹ Fakultät für Mathematik und Naturwissenschaften, Fachgruppe Physik, Bergische Universität Wuppertal, Wuppertal, Germany
¹⁸⁰ Department of Physics, Yale University, New Haven, CT, United States of America
¹⁸¹ Yerevan Physics Institute, Yerevan, Armenia

^a Also at Borough of Manhattan Community College, City University of New York, NY; United States of America.

^b Also at California State University, East Bay; United States of America.

^c Also at Centre for High Performance Computing, CSIR Campus, Rosebank, Cape Town; South Africa.

^d Also at CERN, Geneva; Switzerland.

^e Also at CPPM, Aix-Marseille Université, CNRS/IN2P3, Marseille; France.

^f Also at Département de Physique Nucléaire et Corpusculaire, Université de Genève, Genève; Switzerland.

^g Also at Departament de Física de la Universitat Autònoma de Barcelona, Barcelona; Spain.

^h Also at Departamento de Física, Instituto Superior Técnico, Universidade de Lisboa, Lisboa; Portugal.

ⁱ Also at Department of Applied Physics and Astronomy, University of Sharjah, Sharjah; United Arab Emirates.

^j Also at Department of Financial and Management Engineering, University of the Aegean, Chios; Greece.

^k Also at Department of Physics and Astronomy, University of Louisville, Louisville, KY; United States of America.

^l Also at Department of Physics and Astronomy, University of Sheffield, Sheffield; United Kingdom.

^m Also at Department of Physics, California State University, Fresno CA; United States of America.

ⁿ Also at Department of Physics, California State University, Sacramento CA; United States of America.

^o Also at Department of Physics, King's College London, London; United Kingdom.

^p Also at Department of Physics, St. Petersburg State Polytechnical University, St. Petersburg; Russia.

^q Also at Department of Physics, Stanford University; United States of America.

^r Also at Department of Physics, University of Fribourg, Fribourg; Switzerland.

^s Also at Department of Physics, University of Michigan, Ann Arbor MI; United States of America.

- ^t Also at Giresun University, Faculty of Engineering, Giresun; Turkey.
- ^u Also at Graduate School of Science, Osaka University, Osaka; Japan.
- ^v Also at Hellenic Open University, Patras; Greece.
- ^w Also at Horia Hulubei National Institute of Physics and Nuclear Engineering, Bucharest; Romania.
- ^x Also at Il. Physikalisches Institut, Georg-August-Universität Göttingen, Göttingen; Germany.
- ^y Also at Institutio Catalana de Recerca i Estudis Avancats, ICREA, Barcelona; Spain.
- ^z Also at Institut für Experimentalphysik, Universität Hamburg, Hamburg; Germany.
- ^{aa} Also at Institute for Mathematics, Astrophysics and Particle Physics, Radboud University Nijmegen/Nikhef, Nijmegen; Netherlands.
- ^{ab} Also at Institute for Particle and Nuclear Physics, Wigner Research Centre for Physics, Budapest; Hungary.
- ^{ac} Also at Institute of Particle Physics (IPP); Canada.
- ^{ad} Also at Institute of Physics, Academia Sinica, Taipei; Taiwan.
- ^{ae} Also at Institute of Physics, Azerbaijan Academy of Sciences, Baku; Azerbaijan.
- ^{af} Also at Institute of Theoretical Physics, Ilia State University, Tbilisi; Georgia.
- ^{ag} Also at Instituto de Física Teórica de la Universidad Autónoma de Madrid; Spain.
- ^{ah} Also at Istanbul University, Dept. of Physics, Istanbul; Turkey.
- ^{ai} Also at Joint Institute for Nuclear Research, Dubna; Russia.
- ^{aj} Also at LAL, Université Paris-Sud, CNRS/IN2P3, Université Paris-Saclay, Orsay; France.
- ^{ak} Also at Louisiana Tech University, Ruston LA; United States of America.
- ^{al} Also at LPNHE, Sorbonne Université, Paris Diderot Sorbonne Paris Cité, CNRS/IN2P3, Paris; France.
- ^{am} Also at Manhattan College, New York NY; United States of America.
- ^{an} Also at Moscow Institute of Physics and Technology State University, Dolgoprudny; Russia.
- ^{ao} Also at National Research Nuclear University MEPhI, Moscow; Russia.
- ^{ap} Also at Physics Dept, University of South Africa, Pretoria; South Africa.
- ^{aq} Also at Physikalisches Institut, Albert-Ludwigs-Universität Freiburg, Freiburg; Germany.
- ^{ar} Also at School of Physics, Sun Yat-sen University, Guangzhou; China.
- ^{as} Also at The City College of New York, New York NY; United States of America.
- ^{at} Also at The Collaborative Innovation Center of Quantum Matter (CICQM), Beijing; China.
- ^{au} Also at Tomsk State University, Tomsk, and Moscow Institute of Physics and Technology State University, Dolgoprudny; Russia.
- ^{av} Also at TRIUMF, Vancouver BC; Canada.
- ^{aw} Also at Universidad de Granada, Granada (Spain); Spain.
- ^{ax} Also at Università di Napoli Parthenope, Napoli; Italy.
- * Deceased.